Tactile Perception by Electrovibration

by

Yasemin Vardar

A Dissertation Submitted to the
Graduate School of Sciences and Engineering
in Partial Fulfillment of the Requirements for
the Degree of

Doctor of Philosophy

in

Mechanical Engineering

KOÇ
UNIVERSITY

January, 2018

Tactile Perception by Electrovibration

Koç University

Graduate School of Sciences and Engineering

This is to certify that I have examined this copy of a doctoral dissertation by

Yasemin Vardar

and have found that it is complete and satisfactory in all respects,
and that any and all revisions required by the final
examining committee have been made.

Committee Members:

_____

Prof. Dr. Cagatay Basdogan (Thesis Co-Advisor)

_____

Prof. Dr. Burak Güçlü (Thesis Co-Advisor)

_____

Prof. Dr. J. Edward Colgate

_____

Prof. Dr. Hong Z. Tan

_____

Assoc. Prof. Dr. Ipek Basdogan

_____

Asst. Prof. Dr. Evren Samur

Date: _____

To my beloved family,

To my love

ABSTRACT

One approach to generating realistic haptic feedback on touch screens is electrovibration. In this technique, the friction force is altered via electrostatic forces, which are generated by applying an alternating voltage signal to the conductive layer of a capacitive touchscreen. Although the technology for rendering haptic effects on touch surfaces using electrovibration is already in place, our knowledge of the perception mechanisms behind these effects is limited. This thesis aims to explore the mechanisms underlying haptic perception of electrovibration in two parts. In the first part, the effect of input signal properties on electrovibration perception is investigated. Our findings indicate that the perception of electrovibration stimuli depends on frequency-dependent electrical properties of human skin and human tactile sensitivity. When a voltage signal is applied to a touchscreen, it is filtered electrically by human finger and it generates electrostatic forces in the skin and mechanoreceptors. Depending on the spectral energy content of this electrostatic force signal, different psychophysical channels may be activated. The channel which mediates the detection is determined by the frequency component which has a higher energy than the sensory threshold at that frequency. In the second part, effect of masking on the electrovibration perception is investigated. We show that the detection thresholds are elevated as linear functions of masking levels for simultaneous and pedestal masking. The masking effectiveness is larger for pedestal masking compared to simultaneous masking. Moreover, our results suggest that sharpness perception depends on the local contrast between background and foreground stimuli, which varies as a function of masking amplitude and activation levels of frequency-dependent psychophysical channels.

ÖZETÇE

Dokunmatik ekranlarda gerçekçi his elde etmenin bir yolu elektro-titreşimdir. Bu teknikte, parmakla ekran arasındaki sürtünme kuvveti elektrostatik kuvvetler aracılığıyla değiştirilir. Bu kuvvetler alternatif bir voltaj sinyalinin kapasitif bir dokunmatik ekranın iletken katmanına uygulanmasıyla oluşur. Bu yöntemi kullanarak dokunmatik ekranlarda farklı dokunsal etkiler sağlanılsa da, bu dokunsal etkilerin algılanma mekanizması hakkında kısıtlı bilgi bulunmaktadır. Bu tezin amacı dokunmatik ekranlarda oluşturulan dokunsal etkilerin algılanma mekanizmasının araştırılmasıdır. Bu tez iki kısımdan oluşur. Birinci kısımda, giriş voltaj sinyal özelliklerinin eletro-titreşim algılanmasına etkisi araştırılmıştır. Bulgularımız elektro-titreşim algısının frekansla değişen insan derisi özelliklerine ve insan dokunma hassasiyetine bağlı oldu˘gunu göstermiştir. Ekrana uygulanan giriş voltaj sinyali önce insan derisinde elektiriksel filtrelemeye uğrar, daha sonra ise deride ve mekanoreseptörlerde elektrostatik güç oluşturur. Oluşan gücün spekral enerji bileşenlerine bağlı olarak, farklı psikofizik kanallar uyarılabilir. Algılanmayı sağlayan kanal, o frekansta ölçülen algılanma seviyesinden daha yüksek enerjiye sahip olan frekans bileşeni tarafından belirlenir. İkinci kısımda, maskelemenin elektro-titreşim üzerindeki etkisi araştırılmıştır. Sonuçlarımız, algılama eşiklerinin eşzamanlı ve sürekli maskeleme için maskeleme genliğine bağlı olarak doğrusal fonksiyon şeklinde yükseldiğini göstermiştir. Bununla beraber, sürekli maskeleme etkisi eşzamanlı maskeleme etkisinden daha fazla olmuştur. Ayrıca keskinlik algılaması arka plan ve ön plan uyaranların oluşturduğu lokal kontrasta bağlıdır. Bu kontrast, maskeleme sinyalinin genliği ve frekansa bağlı psikofizik kanal aktivasyon seviyesine göre değişmektedir.

ACKNOWLEDGMENTS

I would like to thank, first and foremost, to my advisors Cagatay Basdogan and Burak Güçlü for their guidance throughout my Ph.D. study. It is very hard to find any words to describe my gratefulness to them. They provided me a great research environment that motivated me to be an independent, curious, analytical, and creative researcher. I have been fed by their different approaches and had an opportunity to develop myself both as an engineer and a scientist. They spent an enormous amount of time and effort to raise me. I will never forget the things they have done for me. I would like to thank Cagatay Basdogan for teaching me to seek always the best. When I think the mistakes I did in past, I admire the patience and faith he showed for me. He always supported me to develop myself beyond my boundaries. Besides, he showed a great patience to my emotional breakdowns and high level of stress. I would like to thank Burak Güçlü for teaching me how to be a good scientist. Thanks to him, I tasted the joy of working on fundamental science.

I would like to thank Prof. Dr. Edward Colgate, Prof. Dr. Hong Tan, Dr. Ipek Basdogan, and Dr. Evren Samur for agreeing to be part of my thesis committee. I would like to thank them for spending their precious time to listen to my presentation and read my thesis. I am very fortunate to benefit from their suggestions and perspectives. Also, I would like to thank Prof. Dr. Ozgur Birer for his valuable comments and discussions in the early phase of this study.

I would like to thank Ozan Caldiran for his valuable comments, and fruitful discussions during my study. His comments about my very first experiments led me to dig in more and understand the physical mechanism behind the electrovibration. He was always the first volunteer to my experiments without any complaints. I wonder if I would be in this situation without his companionship.

I would like to thank Utku Boz, M. Khurram Saleem, Aykut Isleyen, Amir Reza Aghakhani, Yusuf Aydin, and Omer Sirin for their valuable comments and technical help during preparation of the hardware and software needs of my experimental apparatus. Thanks to them, I got critical answers quickly when I stuck, and moved on. They always answered my questions, even my questions were very ridiculous, with a great patience. I was very lucky to have such good colleagues to whom I can ask for help anytime.

I would like to thank Senem Ezgi Emgin and Enes Selman Ege for their initial help and support. They introduced electrovibration to me and provided a quick start for my Ph.D. study. I learned a lot from them and developed my study based on the foundation they provided to me.

I would like to thank Tamara Fiedler, and Aykut Isleyen for being collaborators in my research. When we first met, they were like a sapling I planted. Now, they are like young trees with lots of fruits and flowers. I gained a lot from working together in terms of developing research and management skills.

I would like to thank all subjects who participated in my experiments. They spent enormous time and showed great patience to complete my study voluntarily. I will never forget their self-sacrifice.

I would like to thank my all teachers who educated me since preliminary school. I would not be in this situation without their foundation and efforts. I will never forget any contribution they added to my personality, perspective, and scientific knowledge.

I would like to thank my family. Mom and dad have raised me as a healthy, strong, ambitious, curious and independent woman. They always supported me to follow my dreams and taught me never giving up. My sisters Yesim and Ozlem always listened to me and showed the best path when I lost my way. My grandfather and grandmother always wished the best things for me, and made me feel proud of myself during my long studentship period. Although there are kilometers between us, I have always felt my family standing right next to me. It was always such a relief to have

people on my back regardless of the difficulty of any situation.

I would like to thank Gokhan Serhat for his endless support in this adventure. He has helped me to find my path, happiness, joy, and love again. He has always held my hand when I fell down and cheered me up during my emotional breakdowns. He always motivated me to enjoy life, nature, sports, and science. Also, I gained a lot from his extraordinary intelligence during our discussions about my research.

I would like to thank my friends Buket Baylan, Utku Boz, Mehmet Murat Gozum, Ozan Caldiran, Serena Muratcioglu, Yusuf Aydin, Sinemis Temel, Amir Reza Aghakhani, Isil Koyuncu, Bugra Bayik, Tagra Bayik, Omer Sirin, Mehmet Ayyildiz, Bilgesu Erdogan, Efe Elbeyli, Ipek Karakus, and Yavuzer Karakus for their great friendship. We shared laughter, joy, pain, tears, and frustration together. They were ears when I needed to talk, shoulders when I needed to cry, hands when I needed help, tongues when I needed to be criticized. I feel very lucky to have you in my life. Moreover, I would like to thank my other collogues in RML lab: Cigil Ece Madan, Mohammad Ansarin, Soner Cinoglu, Bushra Sadia, Zaid Rassim Mohammed al-saadi, Yahya Mohey Hamad Al-qaysi, Ayberk Sadic, Utku Erdem, and Milad Jamalzadeh.

The Scientific and Technological Research Council of Turkey (TUBITAK) supported this work under Student Fellowship Program BIDEB-2211.

TABLE OF CONTENTS

LIST OF TABLES

LIST OF FIGURES

NOMENCLATURE

FA	Fast adapting
SA	Slowly adapting
P	Pacinian
NPI-III	Non-Pacinian I- III
ISI	Inter-stimulus interval
F	Electrostatic force between parallel conducting plates
d	Insulator thickness between two conducting plates
V_g	Voltage difference between two conducting plates
ϵ	Permittivity of the insulator between two conducting plates
A_p	Area of the conducting plates
A	Area of the finger pad
ITO	Indium tin oxide
F_e	Electrostatic force on fingertip
ϵ_0	Permittivity of vacuum
ϵ_{sc}	Relative permittivity of stratum corneum
ϵ_{air}	Relative permittivity of air
V	Applied voltage
d_{sc}	Thickness of stratum corneum
d_{air}	Thickness of air gap
Z_{sc}	Impedance of stratum corneum
Z_{air}	Impedance of air gap
Z_i	Impedance of insulator
Z_{body}	Impedance of human body
V_{sc}	Voltage across the stratum corneum

V_{air}	Voltage across the air gap
μ	Friction coefficient
F_n	Applied normal force
F_f	Friction force
R_{body}	Resistance of human body
C_i	Capacitance of insulator
R_{sc}	Resistance of stratum corneum
C_{sc}	Capacitance of stratum corneum
ρ_{sc}	Resistivity of stratum corneum
DAQ	Data Acquisition
IR	Infra-red
EMI	Electromagnetic interference
dB	Decibel
SL	Sensation level
RMS	Root mean square
ANOVA	Analysis of variance
NBN	Narrow band noise
GUI	Graphical user interface
E	Edge
PM1	Pedestal masking 1
PM2	Pedestal masking 2
PM3	Pedestal masking 3
SM1	Simultaneous masking 1
SM2	Simultaneous masking 2
SM3	Simultaneous masking 3
R	Ramped pedestal masking
PML	Pedestal masking low frequency
S1-S9	Subject 1-9

Chapter 1

INTRODUCTION

Touch screens are an indispensable part of our lives. They are used in several electronic devices such as smartphones, tablet computers, smart TVs, kiosks, and digital information panels. The usage of touch screens simplifies the design of the electronic devices into one piece of equipment and ease the tailoring of their user interfaces. However, our interactions with current touchscreens mainly involve auditory and visual channels and lack tactile feedback. Tactile feedback can, for example, improve user performance during gesture interactions with digital controls such as keyboards, sliders, and knobs. Receiving a tactile confirmation when you press a digital key or feeling the detents of a digital knob while rotating it may help to user focus on the task rather than the controller itself. Moreover, providing realistic tactile feedback can enhance user experience and human perception in interactive applications such as online shopping, digital games, and education. For example, feeling the simulated texture of a jean before purchasing it from Internet would certainly be more motivating for shoppers. Furthermore, designing user interfaces for visually impaired so that they can feel the shapes of digital objects and appreciate graphical information on touch screens is another motivating and exciting application.

Currently, there are two main techniques to generate realistic tactile feedback on touchscreens: ultrasonic vibration and electrovibration. In both techniques, tactile sensations are generated by modulating the friction between user fingertip and touchscreen. In the former one, the frictional force is attenuated by mechanical actuation of the touch screen at its ultrasonic resonance frequency [Watabene and Fukui, 1995]. By modulating the vibration amplitude [Winfield et al., 2008], rendering different

tactile effects such as textures [Biet et al., 2008] and key-click [Tashiro et al., 2009] is possible. In the latter one, on the other hand, the friction force is altered via electrostatic forces [Bau et al., 2010], which are generated by applying an alternating voltage signal to the conductive layer of a capacitive touch screen [Mayer et al., 2013]. By changing the amplitude [Bau et al., 2010], frequency [Vezzoli et al., 2014, Mayer et al., 2013] and waveform of the input voltage, it is possible to render textures [Ilkhani et al., 2017, Vardar et al., 2017c] and even 3D shapes [Osgouei et al., 2017] on touch screens. This thesis focuses on the latter technique, electrovibration.

1.1 Problem Definition and Approach

Although electrovibration can potentially provide rich tactile sensations, the number of applications of this technology is limited yet due to our poor understanding of the electrical and mechanical properties of human finger and its interaction with a touch surface. For example, both the electrical and mechanical impedance of the human finger are frequency-dependent, and the coupling between them has not been well understood yet [Bau et al., 2010, Mayer et al., 2013, Vezzoli et al., 2014, Kim et al., 2015]. Moreover, human to human variability of these properties and the influence of the environmental factors on these properties further complicate the problem.

In addition to the physical factors mentioned above, it is known that human tactile (mechanical) perception varies with stimulation amplitude and frequency [Gescheider et al., 2002]. Even though the effects of amplitude and frequency on the human tactile perception of electrovibration have already been investigated using pure sine waves [Bau et al., 2010], there is no earlier study on how our perception changes when another waveform is used.

Moreover, the future touch screen applications probably will include multiple and complex tactile stimuli displayed simultaneously or consecutively to a single finger or multiple fingers. Even though it is quite easy to generate any desired stimuli via electrovibration, there is no study on how our perception is affected when multiple stimuli are displayed simultaneously or consecutively. Previous vibrotactile (i.e. mechanical

stimulation of the skin) studies have shown that presenting one stimulus may interfere with the perception of another one. This interference is called tactile masking and can cause certain deficits in perception such as increasing detection thresholds and hindering localization or identification [Enriquez and MacLean, 2008, Güçlü and Öztek, 2007]. Although the neural mechanisms of tactile masking are not exactly known, they mostly occur centrally by changing the signal-to-noise ratio [Gescheider et al., 2009]. Considering the fact that the interaction area of touch screens is much larger than those used in earlier vibrotactile studies, tactile masking has a greater potential for digital applications utilizing electrovibration. For example, many applications on touchscreens in the future may require tactile display of various geometrical shapes made of vertices, edges, or smooth curves, which may be displayed simultaneously with a background texture [Saga and Raskar, 2013]. As illustrated in Fig. 1.1, background textures, displayed by electrovibration may cause tactile masking of object edges. In addition to the single-touch haptic applications today, gesture-based multi-touch haptic applications will be possible in the future. For example, when rendering a haptic knob on a touch screen, different haptic stimuli can be displayed to each finger of a hand during a rotation gesture (Fig. 1.2a). On the other hand, index fingers of different hands may interact with two sliders on the screen displaying different haptic stimuli (Fig. 1.2b). In such cases, the haptic information delivered to different fingers may be integrated into our brain, within the same hemisphere or between hemispheres, in a complex manner due to interference effects similar to masking [Kuroki et al., 2017]. Moreover, tactile feedback may be in contradiction with visual feedback and cause a perceptual confusion [Ide and Hidaka, 2013]. Obviously, tactile masking on touch screens is even more critical when designing user interfaces for visually impaired [Xu et al., 2012, Güçlü et al., 2014].

The first aim of this thesis is to investigate how input voltage waveform alters human haptic perception of electrovibration. This work is mainly motivated by our initial observation that square-wave excitation causes stronger vibratory sensation than sine-wave excitation. According to the parallel-plate capacitor principle, the

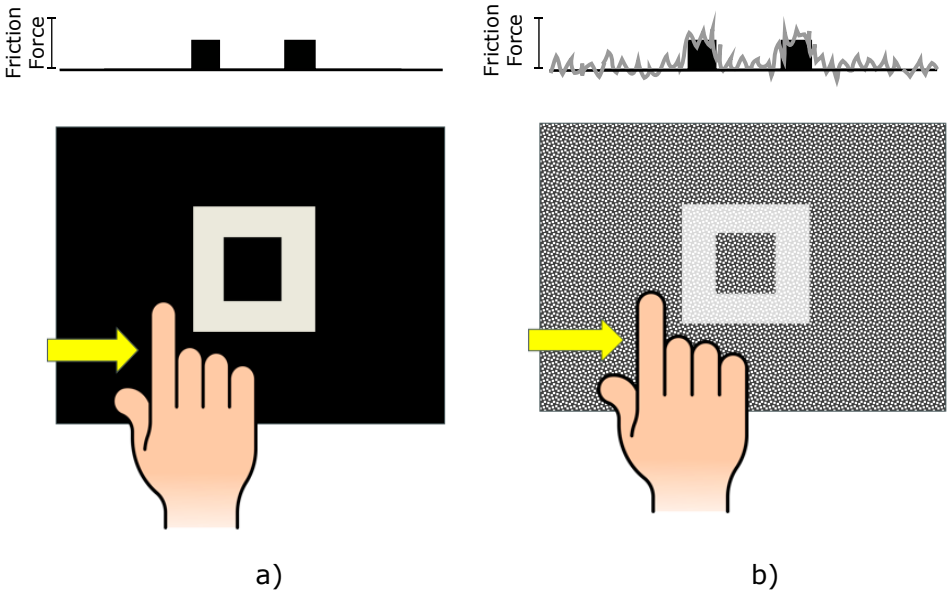

Figure 1.1: Fig 1a. A small square with constant edge thickness is haptically displayed to user by rendering electrovibration at the edges. 1.b. The square is displayed within a noise texture. Due to masking effects, the edges of the square may be perceived less sharper.

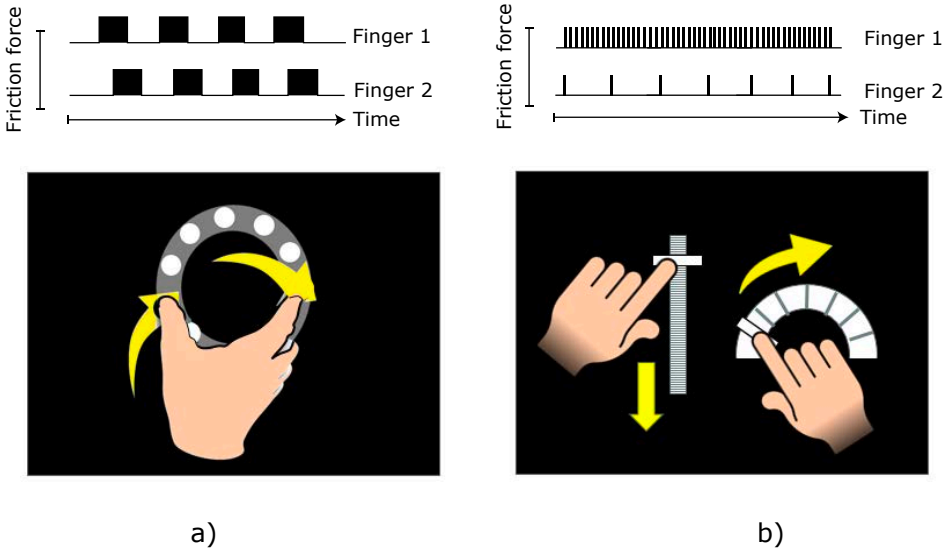

Figure 1.2: Fig 1a. A haptic knob is displayed to a user by rendering electrovibration at its detents. The same tactile stimuli with a phase difference was delivered to both fingers as they rotate the knob. Due to the masking effects, the user may feel detents with less amplitude and without a temporal difference. 1.b. Two haptic sliders are rendered by displaying different electrovibration stimuli to each finger. However, the user may not feel the differences appreciatively due to the interference.

electrostatic force is proportional to the square of the input voltage signal, hence the electrostatic force generated by a square-wave is supposed to be constant [Demarest, 1998]. Since DC (constant) excitation voltages do not cause vibration sensation (though it causes adhesion sensation as reported in [Shultz et al., 2013, Johnsen and Rahbek, 1923]), the square wave excitation is expected to be filtered electrically by the stratum corneum. This filtering suppresses the low-frequency components in the excitation voltage and generates an electrostatic force with a distorted waveform. We hypothesize that the stronger vibratory sensation caused by a square wave is due to the high-frequency components in the resulting force signal. Since this waveform is rather complex (contains many frequency components), it can activate different psychophysical channels at different threshold levels [Bolanowski et al., 1988, Gescheider et al., 2002]. These four psychophysical channels (NPI, NPII, NPIII, P) are mediated by four corresponding mechanoreceptors and enable tactile perception. To predict tactile sensitivity, the Fourier components of the waveform should be analyzed by considering human sensitivity curve [Gescheider et al., 2002].

The second aim of this thesis is to investigate how tactile masking affects the human perception of electrovibration. In the previous masking studies, the tactile stimuli were presented to subjects by vibrotactile actuators such as mechanical shakers [Güçlü and Öztek, 2007], vibrotactile pins [Craig and Evans, 1987], voice coils [Enriquez and MacLean, 2008], and vibration motors [Tan et al., 2003]. These tactile stimuli were delivered to stationary fingers of the subjects and mostly applied in the direction normal to the actuated surface. However, in touch screens actuated by electrovibration, there is almost no feeling when finger is stationary. The haptic effect, which is due to an increase in friction force, is felt by the user only when her/his finger is sliding. Therefore, the effect of masking in electrovibration may be different than mechanical actuation. To explore this, we first measured the detection thresholds of sinusoidal and narrowband noise bursts applied to index fingertips of nine subjects while scanning on the touchscreen. Then, the detection thresholds of sinusoidal bursts were measured with different masking noise stimuli (simultaneous

and pedestal) at sensation levels varied between 2-22 dB SL. Finally, to illustrate how masking can enhance the design of future applications, we investigated the perceived sharpness of the edges separating two textured regions displayed with and without various background noise (similar to Fig. 1.1b).

1.2 Contribution

In this thesis, we investigated tactile perception by electrovibration displayed on touch screens in two parts.

In the first part, using a simulation model developed in Matlab-Simulink, we first show that the forces displayed to human finger by electrovibration are very different for square and sinusoidal input voltages at low fundamental frequencies due to electrical filtering. Then, we show that the force waveform generated by square-wave excitation contains high-frequency components to which human tactile sensation is more sensitive. We support this claim by presenting the results of two experiments conducted with eight subjects. In the first experiment, we measure the detection threshold voltages for sinusoidal and square signals at various frequencies. In the second experiment, we actuate the touch screen at those threshold voltages and measure the contact force and acceleration acting on the index finger of subjects moving on the touch screen with a constant speed. We analyze the collected data in frequency domain by taking into account the human sensitivity curve and show that the square wave excites mainly Pacinian channel [Güçlü and Öztek, 2007, Yıldız et al., 2015]. Our results also suggest that scan speed has a significant effect on measured acceleration and force data and potentially on our haptic perception.

In the second part, we show that the detection thresholds of electrovibration stimuli are elevated as a linear function of masking level in both simultaneous and pedestal masking conditions. We also found that pedestal masking is more effective (i.e. higher threshold shift, and higher slope) than simultaneous masking. The novel application of sharpness perception presented in this thesis was shown to be influenced by masking effect of background texture. Our results suggest that sharpness perception depends

on the local contrast between background and foreground stimuli, and this contrast is a function of both masking amplitude and activation levels of frequency-dependent psychophysical channels. To the best of our knowledge, this is the first detailed psychophysical masking study conducted on touch screens where the stimuli were delivered to subjects while they actively explored the surface.

1.3 Outline

This thesis is presented in five chapters including this introduction and organized as follows.

Chapter 2 is segmented into two parts. In the first part, we review the current literature about human vibrotactile perception that falls within the scope of this thesis. In the second part, we provide an extensive summary of related work on electrovibration.

Chapter 3 investigates the effect of input voltage waveform on our haptic perception of electrovibration on touch screens. First, a theoretical model that explains the detection mechanism of electrovibration stimuli is hypothesized. Then this hypothesis is supported by presenting the results of two experiments. The first experiment focuses on obtaining the psychophysical detection thresholds of electrovibration stimuli generated by sinusoidal and square voltages at various fundamental frequencies. The second experiment, on the other hand, focuses on measuring contact force and accelerations acting on the index fingers of the subjects, when the touch screen is actuated at the threshold voltages estimated in the first experiment.

Chapter 4 investigates the effect of masking on the tactile perception of electrovibration displayed on touch screens by presenting two psychophysical experiments. The first experiment aims to determine the influence of masking amplitude and type on the detection thresholds of electrovibration stimuli generated by a sinusoidal voltage. The second experiment, on the other hand, investigates the effect of tactile masking on our haptic perception of edge sharpness.

Chapter 5 concludes the thesis, summarizes the outcomes and contributions and

suggests possible future directions.

Chapter 2

BACKGROUND

2.1 Human Vibrotactile Perception

The vibrotactile stimulation (i.e. mechanical deformation) activates numerous mechanoreceptors in the skin [Jones and Sarter, 2008]. Depending on the skin property (e.g. hairy or glabrous) different mechanoreceptors respond to mechanical stimulation. In this thesis, we only focus on the glabrous skin as the fingertips consist of only that type.

There are four different mechanoreceptors in glabrous skin: Merkel disks, Ruffini end organ, Meissener Corpuscle, and Pacinian corpuscle (see Fig. 2.1). These receptors are categorized based on the nerve fibers that they are connected: (fast-adapting (FA) or slowly-adapting (SA)) and the size of the receptive fields (small (I) or large (II)) of these fibers [Gescheider et al., 2009, Skedung, 2012]. The fast-adapting nerve fibers produce neural spikes only at the beginning and the end of the stimuli. On the contrary, the slowly-adapting nerve fibers produce neural spikes during the whole stimulation period. The receptive fields are related to spatial acuity: the fibers which have small receptive fields respond with a high spatial acuity. The categorization of the mechanoreceptors based on their adaptation rate and receptive fields is shown in Table 2.1. Each receptor is sensitive to different type of stimuli, for example, Pacinian receptors are most sensitive to vibrations, whereas Merkel receptors are most sensitive to pressure.

According to four channel theory [Güçlü and Öztek, 2007, Gescheider et al., 2002, Gescheider et al., 1982, Gescheider et al., 1983, Gescheider et al., 2002, Gescheider et al., 1994, Hamer et al., 1983], the mechanoreceptors in glabrous skin mediate four psychophysical channels (P, NPI, NPII, NPIII). The evidence from earlier stud-

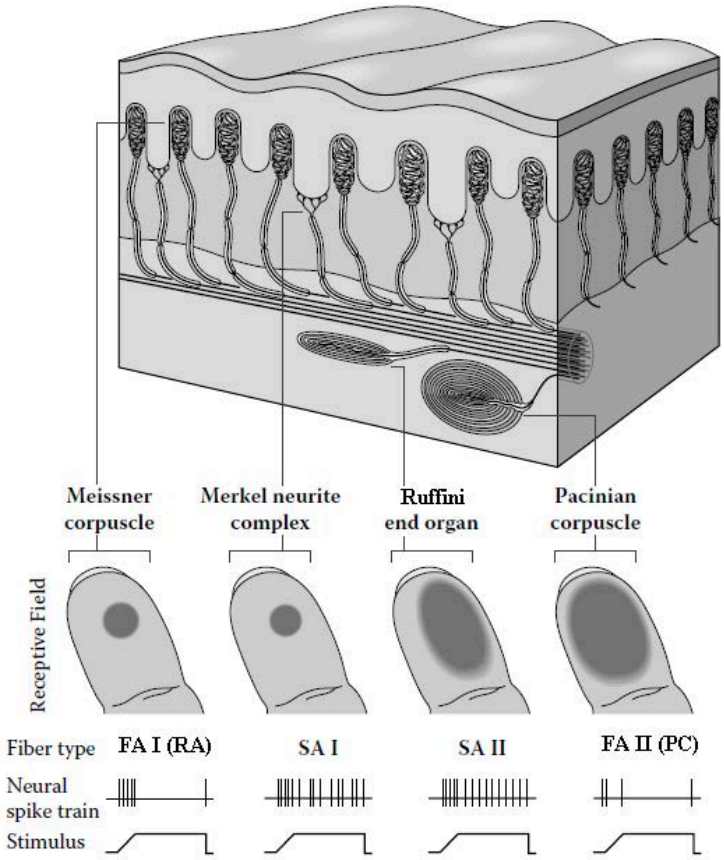

Figure 2.1: Tactile receptors and nerve fibers in glabrous skin [Gescheider et al., 2009].

Table 2.1: The four mechanoreceptors and their response sensitivity [Skedung, 2012]

Mechanoreceptor	**Adaptation Rate**	**Receptive Field**	**Sensitivity**
Merkel Disks	Slow (SA)	Small (I)	Pressure: deformation in spatial structure (2-16 Hz)
Ruffini End Organ	Slow (SA)	Large (II)	Stretch: lateral deformation (100-500 Hz)
Meissener Corpuscle	Fast (FA)	Small (I)	Flutter: light touch, movement or deformation changes (2-40 Hz)
Pacinian Corpuscle	Fast (FA)	Large (II)	Vibration: fine textures, movement or deformation changes (40-500 Hz)

ies suggests that these channels independently process information in the early stages of tactile perception and combine their outputs at later stages within the central nervous system [Gescheider et al., 2009]. Each channel is sensitive to different input frequencies, which partially overlap. The P (Pacinian) channel is mediated by Pacinian receptors, and is most sensitive in the range of 40-500 Hz. Its sensitivity follows a U-shaped trend with a lowest value approximately at 250 Hz. NPII channel shows a similar sensitivity region with P channel, however its sensitivity is much lower than P channel, in case of a large stimulation area. The NPI channel is mediated by Meissener receptors, and it is most sensitive in the range of 2-40 Hz. Finally, the NPIII channel is mediated by Merkel receptors, with a sensitivity region of 2-16 Hz. The sensitivity regions of four channels are illustrated in Fig. 2.2. These sensitive regions were determined in [Gescheider et al., 2001] by conducting detection threshold experiments at various frequencies (0.4-500 Hz) applied to glabrous skin of the hand through a large (2.9 cm^2) and a small (0.008 cm^2) contactors. The detection threshold experiments determine the minimum stimulus amplitude that can be detected. Here, the sensitive frequency regions of the four channels can be seen clearly. The detection thresholds of P channel varies with the contactor size which is due to the spatial summation property of P channel. Among all psychophysical channels, P channel is the only one which has the spatial and temporal summation property. The sensitivity of P channel increases a function of stimulation area (spatial summation) and duration (temporal summation).

2.1.1 Detection of a Complex Vibrotactile Stimulus

A complex vibrotactile stimulus (i.e. mechanical displacement) can be considered as weighted sum of sinusoidal vibrations with different frequencies based on Fourier decomposition [Güçlü and Öztek, 2007]. The tactile detection occurs, when the energy content of one of these sinusoidal vibrations exceeds the detection threshold (energy) at that frequency. In other words, the detection thresholds of a complex vibrotactile stimulus is determined by the spectral component which has the highest energy

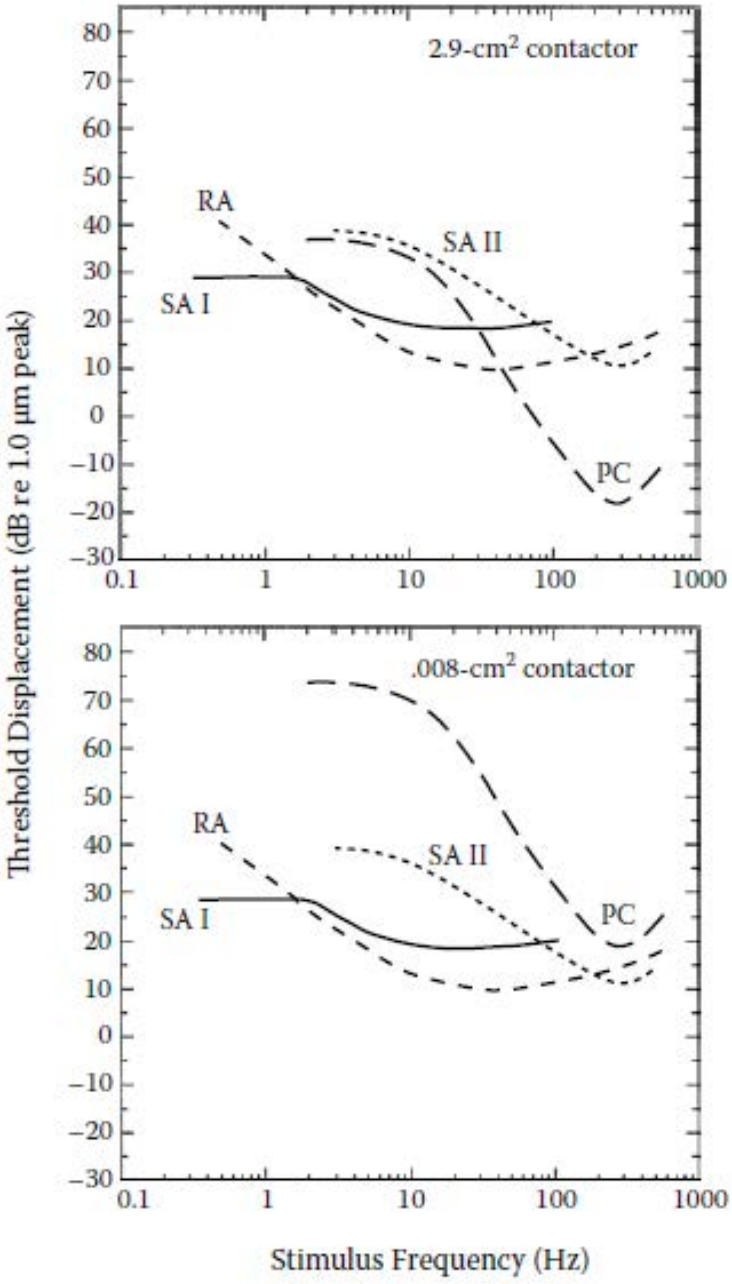

Figure 2.2: The sensitive regions of four psychophysical channels [Gescheider et al., 2001, Gescheider et al., 2009]. These sensitive regions were determined by detection threshold experiments at various frequencies (0.4-500 Hz) applied to glabrous skin of the hand through a large (2.9 cm^2) and a small (0.008 cm^2) contactors. The mechanical stimuli were delivered by actuating a mechanical shaker.

weighted by the human psychophysical sensitivity.

2.1.2 Masking

Human vibrotactile masking has been investigated extensively via detection and identification experiments. In detection experiments, the threshold amplitude for detecting a vibrotactile stimulus is measured separately in the absence of and presence of a masking stimulus. The difference in amplitude is defined as the threshold shift (i.e. amount of masking). In identification experiments, identification performance of a target stimuli in a presence of masking stimuli is determined. The identification of the target stimuli decreases as amount of masking increases. For both detection and identification experiments, the most commonly used masking techniques are forward (masking stimulus precedes test stimulus), backward (masking stimulus follows test stimulus), simultaneous (masking and test stimulus starts and ends at the same time), pedestal (test stimulus occurs during a continuous masking stimulus), sandwich masking (test stimulus is sandwiched between two masking stimuli), and common-onset masking (masking and test stimulus starts simultaneously, but latter one ends earlier). The stimulus timing diagrams of these masking techniques is illustrated in Fig. 2.3.

Researchers have studied vibrotactile masking to understand neural and psychophysical mechanisms behind our touch sensation. The majority of these works were performed by Verrillo and his collogues [Gescheider et al., 1982, Gescheider et al., 1983, Gescheider et al., 2002, Gescheider et al., 1994, Hamer et al., 1983]. They conducted series of detection experiments using pedestal and forward masking techniques. In their experiments, they used test and masking stimuli in wide range of frequencies (0.4 to 500 Hz) applied by contactors in different sizes. The results of these experiments led them put forward the four channel theory explained previously. They found that each channel is sensitive to different input frequencies, which partially overlap. And, tactile masking only occurs when mask and test stimuli excite the same psychophysical channel. Based on these results, they suggested that the perceptual

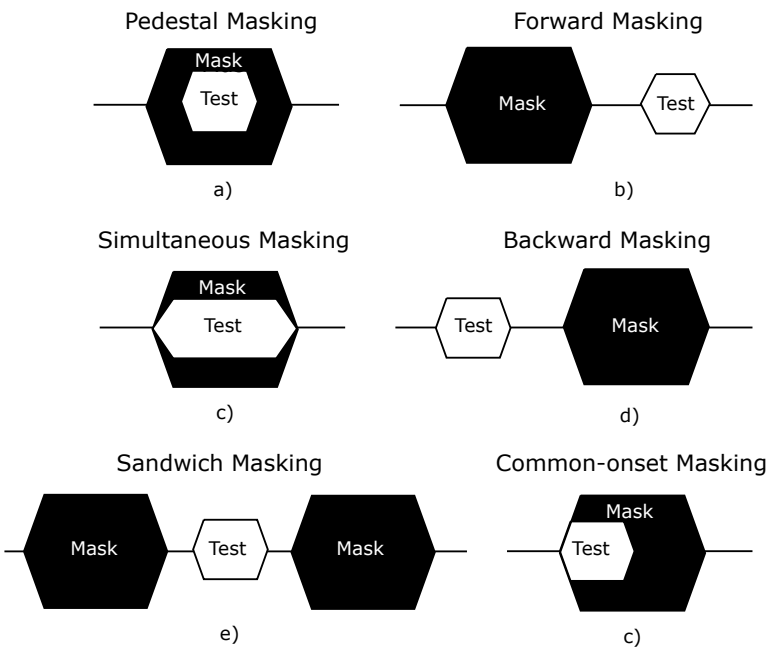

Figure 2.3: Stimulus timing diagrams for a. pedestal, b. forward, c. simultaneous, d. backward, e. sandwich, f. common-onset masking techniques.

qualities of touch might be determined by the combined inputs from four channels. Most of these findings were validated by future works in different laboratories [Makous et al., 1995a, Güçlü and Bolanowski, 2005a, Güçlü and Öztek, 2007], and used in computational modelling of the sense of touch [Güçlü and Bolanowski, 2005b, Güçlü and Bolanowski, 2004, Güçlü et al., 2005, Güçlü, 2007, Güçlü and Ş.M. Dinçer, 2013]. Recently, [Kuroki et al., 2017] applied sinusoidal vibrotactile stimuli in different frequencies to the neighbouring fingers and the different hands of the subjects. When the subjects judged the frequency of one vibration, the perceived frequency shifted towards the other. Moreover, when they judged the frequency of the pair as a whole, they reported the intensity-based interpolation of these two vibrations. These results suggested that perception of frequency is functionally enriched by signal integration across different mechanoreceptor channels and separate skin locations.

Several factors influence the amount of masking. These factors are related to both mask and test stimuli such as their magnitude and duration, as well as the time between them, known as interstimulus interval (ISI). Many studies observed that

increasing the duration of test stimulus and ISI decreases the amount of masking, whereas increasing mask duration and magnitude affect oppositely (see Table 2.2 for summary of these studies). Also, mask site (i.e. applied location on body) is another important factor that affects the resultant masking. The amount of masking increases if the test and mask stimuli applied to the same location [Gilson, 1969, Verrillo and Gescheider, 1983].

Table 2.2: Summary of earlier studies investigating vibrotactile masking.

	Mask Stimuli	**Test Stimuli**	**Mask Level**	**Mask Duration**	**Test Duration**	**ISI**	**Source**
Pedestal	250 Hz sinusoidal & band limited noise (250-1000 Hz)	250 Hz sinusoidal & band limited noise (250-1000 Hz)	Variable 10-50 dB SL	1500 ms	Variable 15-1000 ms	-	[Gescheider et al., 1994]
Forward	500 Hz sinusoidal & centered noise at 27 Hz	500 Hz sinusoidal & centered noise at 27 Hz	Variable 5-25 dB SL	20.5 & 10 ms	20.5 & 10 ms	Variable 5-595 ms	[Makous et al., 1995b]
	20, and 250 Hz sinusoidal	20, and 250 Hz sinusoidal	Variable 10-30 dB SL	Variable 10-1000 ms	50 ms	25 ms	[Gescheider et al., 1995]
	250 Hz sinusoidal	250 Hz sinusoidal	20 dB SL	700 ms	Variable 30- 660 ms	Variable 10-660 ms	[Gescheider and Migel, 1995]
Backward Pedestal Forward	250 Hz sinusoidal	250 Hz sinusoidal	20 dB SL	700 ms	50 ms	Variable 0-2000 ms	[Gescheider et al., 1989]

2.2 Electrovibration for Tactile Displays

2.2.1 Foundation

The electrical attraction between human skin and a charged surface was first reported by [Johnsen and Rahbek, 1923]. Around thirty years later, Mallinckrodt discovered that applying alternating voltages to an insulated aluminum plate can increase friction during touch and create a strange resin-like feeling [Mallinckrodt et al., 1953]. He explained this phenomenon based on the well-known principle of parallel-plate capacitor. Later, Grimnes named this phenomenon as "electrovibration" and reported that surface roughness and dryness of finger skin could affect the perceived haptic effects [Grimnes, 1983a]. Afterwards, [Strong and Troxel, 1970] developed an electrotactile display consisting of an array of electrodes insulated with a thin layer of dielectric. Using friction induced by electrostatic attraction force, they generated texture sensations on the touch surface. Their experimental results showed that the intensity of touch sensation was primarily due to the applied voltage rather than the current density. [Beebe et al., 1995], developed a polyimide-on-silicon electrostatic fingertip tactile display using lithographic microfabrication. They were able to generate tactile sensations on this thin and durable display using 200-600 V voltage pulses and reported the perception at the fingertip as sticky. Later, [Tang and Beebe, 1998] performed experiments of detection threshold, line separation and pattern recognition with visually impaired subjects. Although they encountered problems such as dielectric breakdown and sensor degradation, the subjects were able to differentiate simple tactile patterns by haptic exploration.

In all of the above studies, electrovibration was obtained using opaque patterns of electrodes on small scale surfaces. However, in the recent work of [Bau et al., 2010], electrovibration was delivered via a transparent electrode on a large commercial touch surface, which demonstrates the viability of this technology on mobile applications (see Fig. 2.4c). In this technique, the input voltage signal is sent through a single electrode which causes a uniform feeling all over the touch surface. Later, [Nakamura and

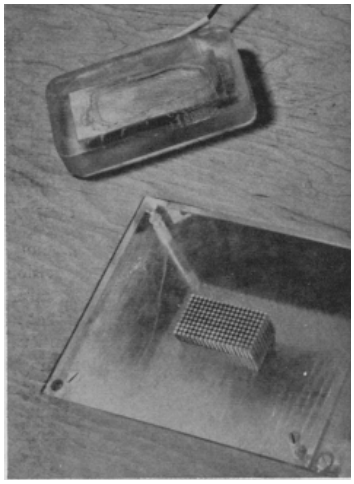

(a) [Strong and Troxel, 1970]

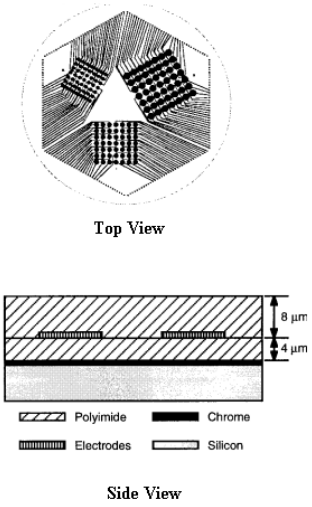

(b) [Tang and Beebe, 1998]

(c) [Bau et al., 2010]

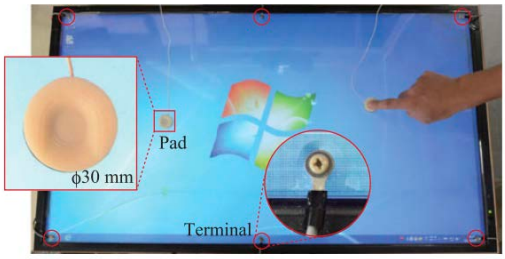

(d) [Nakamura and Yamamoto, 2016]

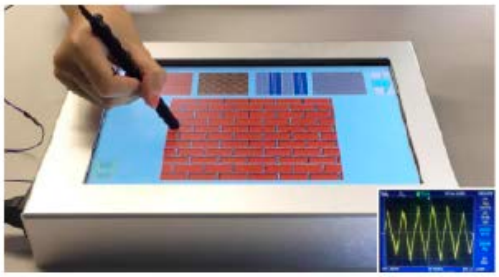

(e) [Wang et al., 2016]

Figure 2.4: Review of the electrostatic display technologies. a. The first electrostatic tactile display. It consists of a matrix of 180 electrodes, insulated with a thin layer of dielectrics. b. A micro-fabricated electrostatic tactile display. The display consists of 7x7 electrode arrays of three different sizes fabricated on a 4-in wafer. c. The first electrostatic system which is displayed on a large and transparent electrode. d. The multi-user surface visuo-haptic display system. The system combines the multi-user electrostatic haptic feedback system and a built-in sensing system employing surface-capacitive-type position sensing. The haptic feedback is enabled by sending voltage input to individual pads. e. EV-pen system. The haptic feedback is generated between the pen and the surface.

Yamamoto, 2016], improved this approach and designed a multi-user surface visuo-haptic display (see Fig. 2.4d). In that study, they delivered the haptic actuation signal to the multiple contact pads instead of the touch surface itself. They applied low-frequency haptic voltage and high-frequency sensing voltage to each pad. In addition to delivering different sensations to multi-fingers, their technique also allowed sensing the finger position without additional hardware. In addition to these approaches, a pen-based electrostatic system (EV-Pen) was introduced by [Wang et al., 2016]. In their system, the input voltage signal is applied to a capacitive pen, and the electrostatic force is generated between the moving pen and the capacitive touch screen (see Fig. 2.4e).

2.2.2 Potential Applications

Electrovibration has potential to be used in many applications. One of the potential applications is texture rendering. The first attempt in this area was done by [Yamamato et al., 2006]. The authors developed a tactile tele-presentation system consisting of a linear stage with a built-in tactile sensor driven as a slave system that moves in synchronization with a slider on the tactile display. The vibration data collected by a tactile sensor is processed and regenerated on tactile display simultaneously via electrovibration. Their experimental results showed that subjects discriminated different textures with a correct response of 79%. Later, [Ilkhani et al., 2017] presented a data-driven haptic rendering method applied to a touchscreen. They collected surface data from real textures using an accelerometer and then replayed on the touchscreen. The results of the psychophysical experiments demonstrated that virtual textures generated by data-driven approach show higher similarity to realistic textures in comparison to the ones generated by periodic square waves in different frequencies. Recently, [Vardar et al., 2017c] designed virtual textures by using low frequency unipolar pulse waves in different shape (sinusoidal, square, sawtooth, triangle), and spacing (e.g. groove width). They modulated these waves with a 3kHz high frequency sinusoidal carrier signal. Their user study showed that roughness percep-

tion followed an inverted U-shaped trend along groove width. The subjects perceived square wave as the roughest while they perceived other waveforms similar.

Another potential application for electrovibration usage is diplaying 3D geometric shapes. The first study on displaying 3D geometric features was done by [Kim et al., 2013]. They developed an algorithm to render a 3D geometrical surface in the form of a height map. For that purpose, they modulated the friction force based on the local gradient of the surface. Following this study, [Osgouei et al., 2017], generalized this algorithm to estimate the surface gradient for any 3D mesh and added an edge detection algorithm to render sharp edges. They tested their algorithm and found that their approach can improve the performance of 3D shape recognition when visual information is limited.

Electrovibration can also be used to develop tools for visually impaired. [Xu et al., 2012] developed applications for visually impaired to interpret and create 2D tactile information using electrovibration. They displayed dots, Braille letters, and shapes by modulating the amplitude and frequency of the input voltage signals. The subjects recognized the dots easily, but had difficulties to recognize the letters. They were moderately successful in recognizing the shapes as well.

2.2.3 Modelling

The electrostatic force developed between a sliding finger and the electrode can be explained by the well-known parallel plate capacitor principle, [Strong and Troxel, 1970], [Kaczmarek et al., 2006]. According to this principle, if two charged conducting parallel plates are separated by an insulator with a thickness d, an electrostatic force, F, occurs across the insulator:

$$F = \frac{\epsilon A_p V_g^2}{2d^2}, \tag{2.1}$$

where ϵ is the permittivity of the insulator, A_p is the area of the conductors, and V_g is the voltage difference between the two conducting layers. Regarding finger-surface

interaction, this model should be modified. A touchscreen used for electrovibration consists of two thin layers deposited on a glass substrate. The first layer on top of the glass is a thin layer of transparent conductive material - mostly indium tin oxide (ITO). On top of this layer, a thin layer of insulator material appears. The fingertip has approximately 200 microns thick outermost skin called stratum corneum. This layer acts as an additional dielectric which enables a potential drop from ITO to the conducting tissue under the stratum corneum when a voltage applies, [Kaczmarek et al., 2006, Mayer et al., 2013, Vezzoli et al., 2014]. Electrostatic forces are developed at the boundaries of the two dielectrics: stratum corneum and insulator. If a human finger on a touchscreen surface is represented in Figure 2.5a, the electrostatic force which effects the fingertip can be expressed as

$$F_e = \frac{\epsilon_0 \epsilon_{sc} A}{2} \left(\frac{V_{sc}}{d_{sc}} \right)^2, \tag{2.2}$$

where ϵ_{sc} is the relative permittivity of the stratum corneum, ϵ_0 is the permittivity of vacuum, A is the area of the fingerpad, d_{sc} is the thickness of the stratum corneum. V_{sc} is the voltage across the stratum corneum, which can be expressed as a function of the voltage applied to the conductive layer of the touch screen, V, as

$$V_{sc} = V \frac{Z_{sc}}{Z_{body} + Z_{sc} + Z_i}, \tag{2.3}$$

where, Z_{body}, Z_{sc}, and Z_i represent the impedances of the human body, stratum corneum, and touch surface respectively. The reader may refer to [Demarest, 1998] for more information related to the derivation of the electrostatic force generated at the boundaries of two parallel or series dielectrics.

Recently, some studies suggest that the air gap between fingertip ridges and touch screen has also great influence on the generated electrostatic force, especially when the voltage input is not alternating (electroadhesion). These studies [Shultz et al., 2013, Nakamura and Yamamoto, 2017] explain that the effective electrostatic force is

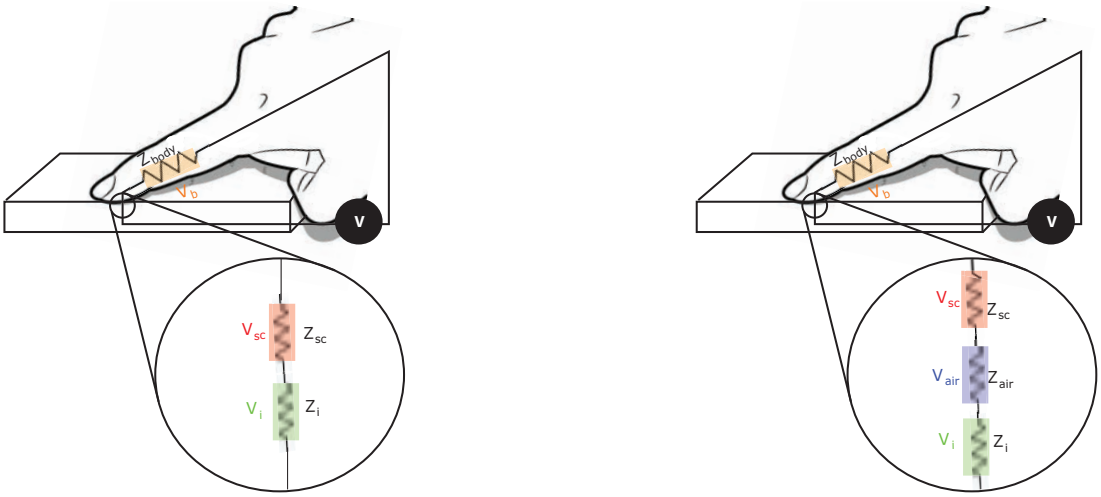

Figure 2.5: Equivalent circuit model of human finger on a tactile display surface: a. neglecting the air gap between finger ridges and touch screen, b. considering the air gap between finger ridges and touch screen.

developed across the thin gap of air at the interference:

$$F_e = \frac{\epsilon_0 \epsilon_{air} A}{2} \left(\frac{V_{air}}{d_{air}} \right)^2, \tag{2.4}$$

where ϵ_{air} is the relative permittivity of the air, d_{air} is the thickness of the air gap. V_{air} is the voltage across the air gap, which can be expressed as a function of the voltage applied to the conductive layer of the touch screen, V, as

$$V_{air} = V \frac{Z_{air}}{Z_{body} + Z_{sc} + Z_{air} + Z_i}, \tag{2.5}$$

where, Z_{air}, represent the impedances of the air (see Fig. 2.5b). Although the effect of air gap on electrovibration has not been validated experimentally yet, according to the results of FEM analysis conducted by [Vodlak et al., 2016] presence of the air gap can increase the electrostatic force up to 10-20 %.

A detailed electromechanical model linking the electrostatic force generation at the fingertip and the mechanical forces of movement has not been developed yet.

However, the contribution of the electrostatic force to the total frictional force F_f is assumed to be Coulombic as:

$$F_f = \mu(F_n + F_e), \tag{2.6}$$

where F_n is normal force applied by the fingertip, and μ is the friction coefficient [Kaczmarek et al., 2006, Mayer et al., 2013, Vezzoli et al., 2014].

To understand how mechanical forces develop at fingertip-surface interface, [Mayer et al., 2013], developed a tribometer and measured the lateral force to estimate the electrostatic attraction force for the applied voltage. They showed the effect of actuation frequency on the lateral frictional force despite some subject-dependent variability. They reported that this person to person variability highly depends on varying environmental impedances caused by voltage controlled electrovibration. Recently, [Kim et al., 2015], suggested a method based on current control to solve the nonuniform intensity problem and developed a hardware prototype working with this principle. The results of their user study showed that the proposed current control method can provide more uniform intensity of electrovibration than voltage controlled one.

2.2.4 Perception

In this section, the previous studies, which investigated the factors affecting electrovibration perception, are reviewed.

Input Signal Properties

The first detailed study which investigated the effect of input signal properties on electrovibration perception was [Kaczmarek et al., 2006]. In that study, the differences in detection for positive, negative and biphasic input voltages was explored. The authors found that the subjects perceived negative or biphasic pulses better than positive ones. They claimed that this disparity could be due to the asymmetric electrical properties of human skin. Later, the sensory thresholds of electrovibration

using sinusoidal inputs applied at different frequencies were measured in [Bau et al., 2010]. The results showed that the change in threshold voltage as a function of frequency followed a U-shaped curve similar to the one observed in vibrotactile studies. In line with these studies, [Wijekoon et al., 2012] investigated the perceived intensity of modulated friction generated by electrovibration. Their experimental results showed that the perceived intensity was logarithmically proportional to the amplitude of the applied voltage signal. Recently, [Kang et al., 2017] investigated the methods that can provide high-intensity electrovibration perception with a lower voltage input. Their force measurements showed that applying input voltage with a DC-offset can provide larger electrostatic force than that of without a DC-offset, when the peak-to-peak amplitudes of both signals are equal. Moreover, their psychophysical experimental results also validated that this method can provide a high-intensity electrovibration perception with less voltage.

Finger Moisture

Although there are not any detailed study on the relation of finger moisture and electrovibration perception, many studies reported that moisture decreases the strength of electrovibration perception [Grimnes, 1983a, Tang and Beebe, 1998, Mallinckrodt et al., 1953]. When a sweat layer accumulates between a fingertip and a touchscreen, the electric field is formed between the touchscreen and the sweat. This situation may decrease the perceived force on the skin. In addition to this, the physical characteristics of sweat layer may also prevent the formation of shear force between fingertip and touchscreen, and degrade the sensation [Tang and Beebe, 1998, Mallinckrodt et al., 1953].

Insulator Properties

[Agarwal et al., 2002] investigated the effect of dielectric thickness on haptic perception during electrostatic stimulation. Their results showed that variations in dielectric thickness had little effect on the threshold voltage.

Chapter 3

EFFECT OF WAVEFORM ON TACTILE PERCEPTION BY ELECTROVIBRATION

Summary

In this chapter[1], we investigated the effect of input voltage waveform on our haptic perception of electrovibration on touch screens. Through psychophysical experiments performed with eight subjects, we first measured the detection thresholds of electrovibration stimuli generated by sinusoidal and square voltages at various fundamental frequencies. We observed that the subjects were more sensitive to stimuli generated by square wave voltage than sinusoidal one for frequencies lower than 60 Hz. Using Matlab simulations, we showed that the sensation difference of waveforms in low fundamental frequencies occurred due to the frequency-dependent electrical properties of human skin and human tactile sensitivity. To validate our simulations, we conducted a second experiment with another group of eight subjects. We first actuated the touch screen at the threshold voltages estimated in the first experiment and then measured the contact force and acceleration acting on the index fingers of the subjects moving on the screen with a constant speed. We analyzed the collected data in the frequency domain using the human vibrotactile sensitivity curve. The results suggested that Pacinian channel was the primary psychophysical channel in the detection of the electrovibration stimuli caused by all the square-wave inputs tested in this study. We also observed that the measured force and acceleration data were affected by finger speed in a complex manner suggesting that it may also affect our haptic perception accordingly.

---

[1]This chapter is based on an article [Vardar et al., 2017a].

3.1 Waveform Analysis of Electrovibration

To investigate the effect of waveform in electrovibration, we developed an equivalent circuit model of human finger in Matlab-Simulink environment. In this model, we neglected the capacitance of the human body and air gap[2] and also the internal resistance of the touch screen (see Fig. 3.1). The capacitance of the touch screen was calculated based on the properties of a commercial touch screen (3M Inc.), which was also used in our experiments[3]. Previous studies showed that the human skin (especially sweat ducts and the stratum corneum) is not a perfect dielectric and has frequency-dependent resistive properties [Kaczmarek et al., 2006, Grimnes, 1983b, Yamamoto and Yamamoto, 1976, Kaczmarek et al., 1991]. Therefore, we modelled stratum corneum as a resistance and a capacitance in parallel. In [Vezzoli et al., 2014], Vezzoli et al. used frequency-dependent values of resistivity, ρ_{sc}, and dielectric constant, ϵ_{sc}, of human stratum corneum reported by [Yamamoto and Yamamoto, 1976]. Their simulations showed that intensity of electrovibration was highly frequency-dependent. Similarly, we fitted polynomial functions to the experimental data reported by [Yamamoto and Yamamoto, 1976] and used those functions in our Matlab simulations (see Fig. 3.2).

Fig. 3.3 represents the Bode plot of the transfer function $\frac{V_{sc}(s)}{V(s)}$, estimated by using the values tabulated in Table 3.1. The system displays the behavior of a bandpass filter with cut-off frequencies, f_{low}, and, f_{high}, at approximately 1 kHz and 20 kHz respectively. Hence, it shows a first order high pass filter behaviour up to 1kHz, which can cause distortions on the voltage that is transmitted to stratum corneum at low frequencies.

To test the effects of this electrical filtering, we performed simulations with two different input waveforms (sinusoidal and square) at two fundamental frequencies

[2]The presence of air gap affects the generated electrostatic force mostly magnitude-wise.

[3]This touch screen is originally designed for capacitive-based touch sensing and composed of a transparent conductive sheet coated with an insulator layer on top of a glass plate. To generate haptic effects via electrovibration, the conductive sheet is excited by applying a voltage signal through the connectors designed for position sensing [Bau et al., 2010].

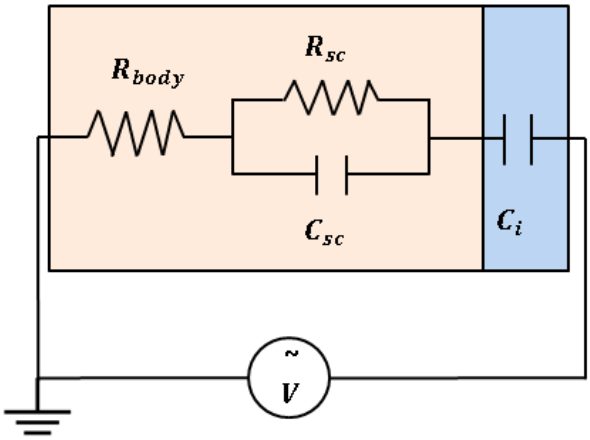

Figure 3.1: The simplified equivalent circuit model of human finger on a touch surface.

Table 3.1: The description of the parameters used in the circuit model and the corresponding values used in the Matlab simulations.

Parameter	**Explanation**	**Value**	**Unit**
A	Area of the human fingertip	1	cm^2
ϵ_0	Permittivity of vacuum	8.854×10^{-12}	F/m
R_{body}	Resistance of human body [Kim et al., 2015]	1	$k\Omega$
C_i	Capacitance of the 3M MicroTouch	$C_i = \frac{\epsilon_0 \epsilon_i A}{d_i}$	F
ϵ_i	Relative permittivity of the insulator	3.9	-
d_i	Thickness of the insulator	1	μm
R_{sc}	Resistance of stratum corneum	$R_{sc} = \frac{\rho_{sc} d_{sc}}{A}$	Ω
C_{sc}	Capacitance of stratum corneum	$C_{sc} = \frac{\epsilon_0 \epsilon_{sc} A}{d_{sc}}$	F
ρ_{sc}	Resistivity of stratum corneum	Fig. 3.2	Ωm
ϵ_{sc}	Relative permittivity of the stratum corneum	Fig. 3.2	-

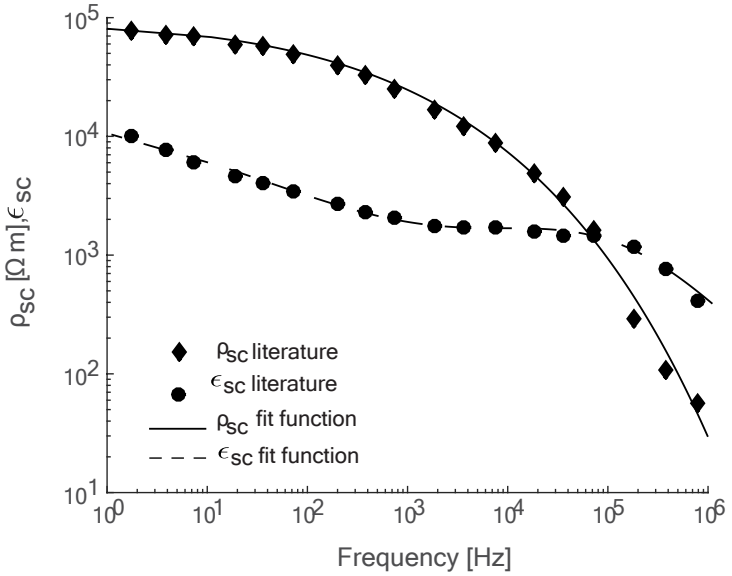

Figure 3.2: The experimental values of resistivity and dielectric constant of stratum corneum as reported in [Yamamoto and Yamamoto, 1976] and the polynomial functions fitted to them.

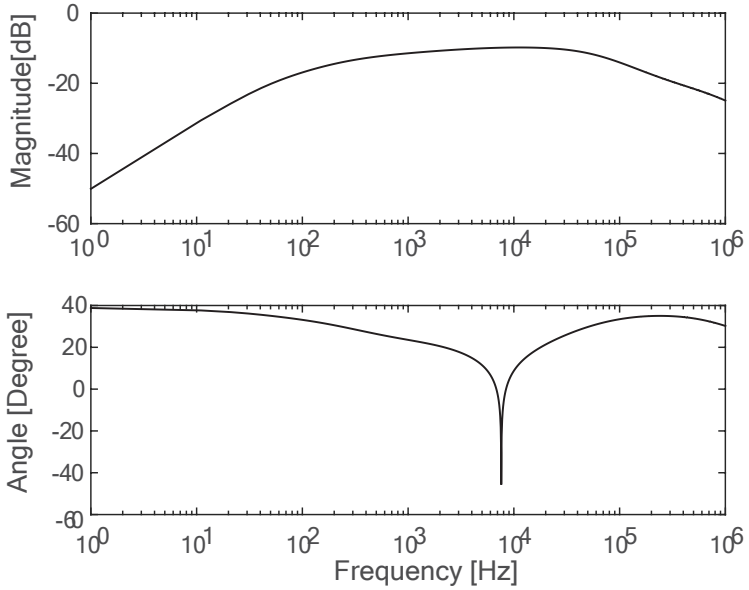

Figure 3.3: The transfer function between V_{sc} and V.

(15 and 480 Hz). Fig. 3.4 shows the input voltage signal, the voltage across stratum corneum (filtered signals), and the resultant electrostatic force transmitted to mechanoreceptors for both waveforms at low and high frequencies (Figs. 3.4a and 3.4b). In low-frequency case (15 Hz), when the input is a sinusoidal signal, the output force signal is phase-shifted, and its amplitude drops significantly. Whereas, for a square wave signal, the output contains exponentially decaying relatively higher amplitude transients. In the high-frequency case (480 Hz), the decline in the output amplitude of the sinusoidal signal is much less, as expected from high pass filtering. Also, the output of the square signal resembles the input signal more because the signal alternates faster than the discharge rate of the capacitor formed by the human skin and touch screen insulator. The results depict that the stimuli on the mechanoreceptors have different waveform and amplitude than those of the input voltage signal.

If a complex waveform (containing many frequency components) arrives at mechanoreceptors, it can activate different psychophysical channels at different threshold levels [Bolanowski et al., 1988, Gescheider et al., 2002, Aiello, 1998]. These four psychophysical channels (NPI, NPII, NPIII, P) are mediated by four corresponding mechanoreceptor populations, which enable the tactile perception[Gescheider et al., 2002, Bolanowski et al., 1988, Güçlü and Bolanowski, 2003, Güçlü and Öztek, 2007, Yıldız and Güçlü, 2013]. For this reason, the Fourier components of the stimulus should be weighted with the inverse of the human sensitivity curve to predict tactile sensitivity to complex stimuli [Gescheider et al., 2002]. The stimulus detection occurs at the channel where the maximum of this weighted function is located in the frequency domain. For example, a sinusoidal signal contains a single frequency component. To be able to detect this signal, its energy level must be higher than the human sensation threshold at that frequency. However, a square signal contains many frequency components. Detection occurs as soon as the energy level of one frequency component is higher than the human sensation threshold at that frequency. The tactile detection process for electrovibration is illustrated in Fig. 3.5. Here, a si-

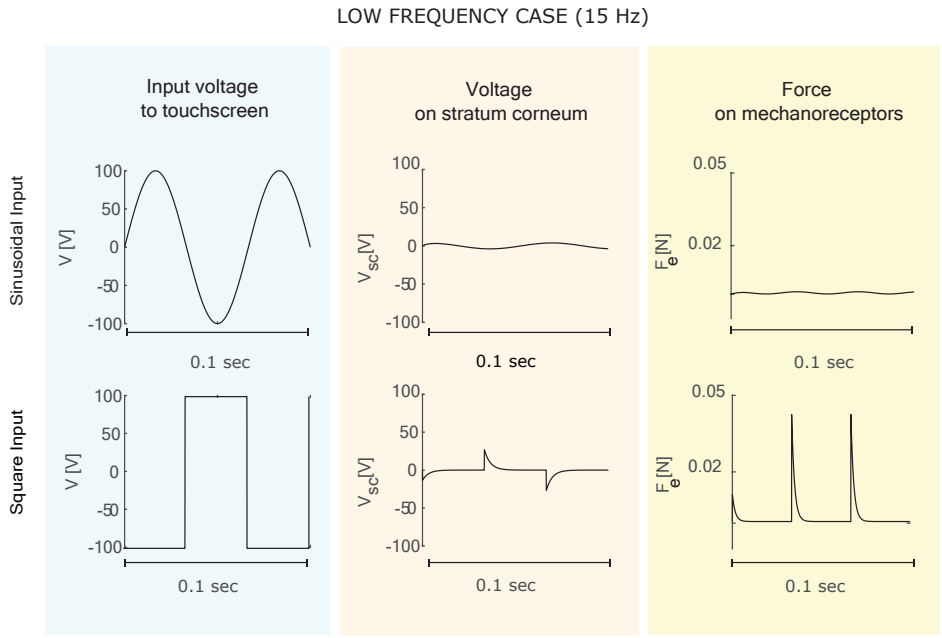

(a)

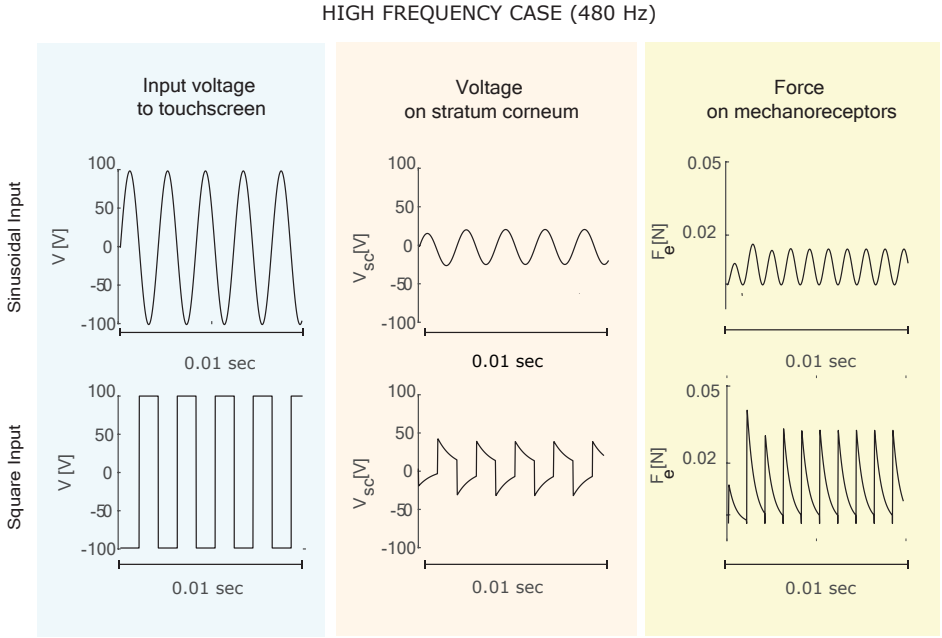

(b)

Figure 3.4: Simulation results: a. low frequency case, b. high frequency case.

nusoidal and a square voltage signals at the same fundamental frequency but different amplitude are applied to the touch screen. Due to electrical filtering of human finger, they generate electrostatic forces on the mechanoreceptors with the *same* amplitude. Therefore, the energy in 30 Hz component is the same for both force signals shown in Fig. 3.5c. However, the square wave input has higher frequency components, which are weighted more with respect to the human sensitivity curve (Fig. 3.5d). As a result, the weighted force signal contains a relatively high frequency component of 180 Hz (Fig. 3.5e). Therefore, in this illustration, the square wave is detected, but the sinusoidal wave is not.

3.2 Materials and Methods

3.2.1 Experiment 1: Psychophysical Experiments

To investigate how our detection threshold changes with input waveform, we conducted absolute detection experiments. These experiments enable us to determine the minimum voltage amplitude that the observer can barely detect [Ehrenstein and Ehrenstein, 1999, Güçlü and Bolanowski, 2005a, Yıldız and Güçlü, 2013, Güçlü and Öztek, 2007]. We aim to compare detection thresholds for sinusoidal and square wave voltage inputs at different frequencies to support our arguments made in Section 3.1.

Participants

We performed experiments with eight subjects (four female, four male) having an average age of 27.5 (SD: 1.19). All of the subjects were right-handed except one. All of them were engineering Ph.D. students. The subjects used the index finger of their dominant hand during the experiments. They washed their hands with soap and rinsed with water before the experiment. Also, their fingers and the touch screen were cleaned by alcohol before each measurement. The subjects read and signed the consent form before the experiments. The form was approved by Ethical Committee for Human Participants of Koç University.

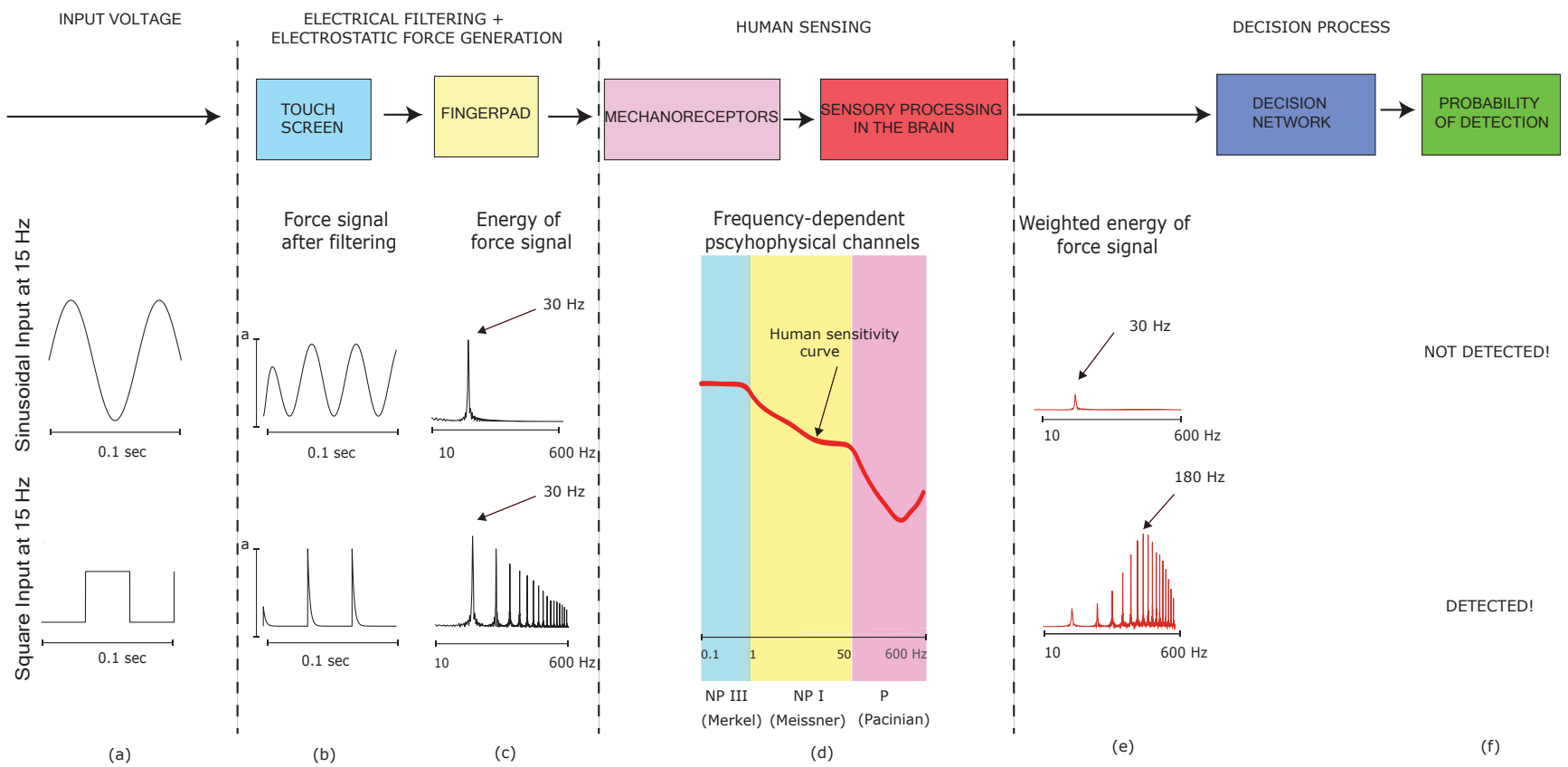

Figure 3.5: An illustration of how tactile detection occurs. a. Input sinusoidal and square voltage signals at 15 Hz applied to touch screen at different amplitudes. b. These input signals are filtered electrically by human finger (see Fig. 3 for filtering process) before generating electrostatic forces with the *same* amplitude on the mechanoreceptors. c. The energy of the force signal originated from the sinusoidal wave contains only one frequency component (30 Hz due to squaring in Equation 2.2) while the one from the square wave contains many frequency components. d. The frequency-dependent human sensitivity curve; the most sensitive frequency regions of three psychophysical channels are color-coded. The fourth channel (NPII) does not appear in this illustration. e. When the Fourier components of the force signals are weighted by the inverse of the human sensitivity curve, the resulting signals from the sinusoidal and square waves have their maximum peaks at 30 and 180 Hz, respectively. Moreover, the energy of the frequency component for the square wave case is larger than that of the sinusoidal one at those frequencies. f. Therefore, the square signal is detected, but the sinusoidal signal is not.

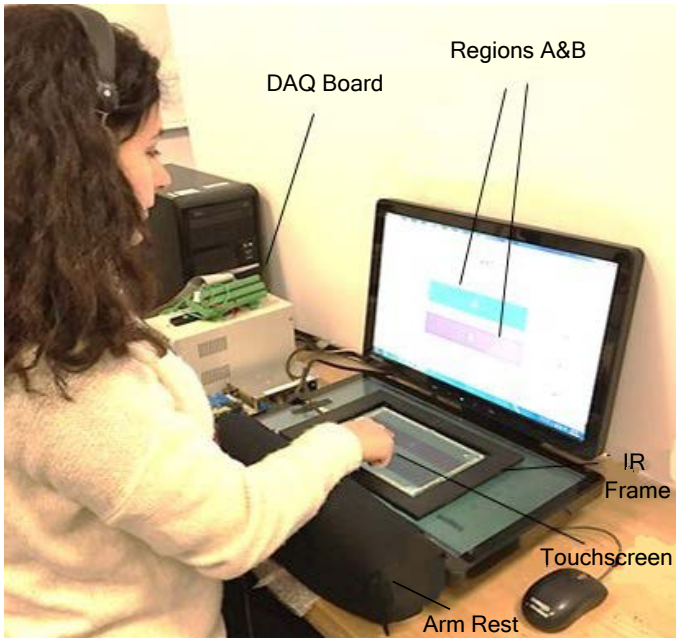

Figure 3.6: Experimental setup used in our psychophysical experiments.

Stimuli

We estimated absolute detection thresholds for seven input frequencies (15, 30, 60, 120, 240, 480 and, 1920 Hz) and two waveforms (sinusoidal and square).

Experimental Setup

The experimental setup used for the psychophysical experiment is shown in Fig. 3.6. A touch screen (SCT3250, 3M Inc.) was placed on top of an LCD screen. An IR frame was placed above the touch screen to detect the finger location. The touch screen was excited with a voltage signal generated by a DAQ card (PCI-6025E, National Instruments Inc.) and augmented by an amplifier (E-413, PI Inc.). Subjects entered their responses through a computer monitor. An arm rest supported the subjects' arms during the experiments. For isolation of the background noises, subjects were asked to wear headphones displaying white noise during experiments.

Procedure

We used the two-alternative-forced-choice method to determine the detection thresholds. This method enables criterion-free experimental results [Güçlü and Öztek, 2007]. We displayed two regions (A and B) on the LCD screen (Fig. 3.6). Tactile stimulus was displayed in only one of the regions, and its location was randomized. The finger position of the subjects was detected via the IR frame. The subjects were asked to explore both areas consecutively and choose the one displaying a tactile stimulus.

We changed the amplitude of the tactile stimulus via one-up/two-down adaptive staircase method. This procedure decreases the duration of the experimentation by reducing the number of trials [Güçlü and Öztek, 2007, Güçlü and Bolanowski, 2003, Yıldız and Güçlü, 2013, Levitt, 1971, Leek, 2001]. We started each session with the stimulus amplitude of 100 V. This initial voltage amplitude provided sufficiently high-intensity stimulus for all the subjects. The voltage amplitude of the new stimulus was adjusted adaptively based on the past responses of each subject. If the subject gave two consecutive correct answers, the voltage amplitude was decreased by 10 V. If the subject had one incorrect response, the stimulus intensity was increased by 10 V. The change of the response from correct to incorrect or the vice versa was counted as one reversal. After four reversals, the step size was decreased by 2V to obtain a more precise threshold value, as suggested in [Bau et al., 2010]. We stopped the experiment after 18 reversals and estimated the absolute detection threshold as the average of the last 15 reversals (Fig. 3.7). The subjects completed the experiments in 14 sessions, executed in 7 separate days (two sessions per day). The duration of each session was about 15-20 minutes.

3.2.2 Experiment 2: Force & Acceleration Measurements

We measured the contact forces and accelerations acting on subjects' finger moving on the surface of the touch screen, which was actuated at the threshold voltages estimated in Experiment 1. Our main goal was to determine the frequency components of these recorded signals in order to validate our theoretical model and simulation results.

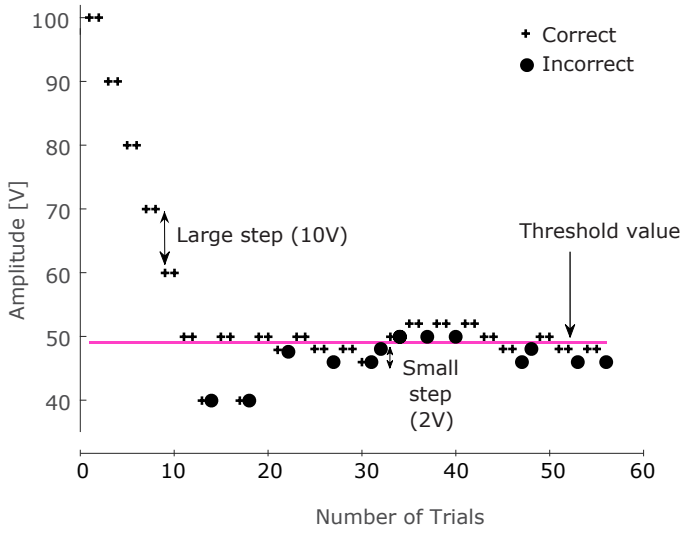

Figure 3.7: An example data set collected by one up-two down adaptive staircase method.

We calculated the signal energies and weighted them with human sensitivity curve to estimate which components enabled the tactile detection. We also investigated the effect of scan speed on measured signals.

Participants

We conducted experiments with eight (four female and four male) subjects having the average age of 27.8 (SD: 2.1). The subjects read and signed the consent form before the experiments. The form was approved by Ethical Committee for Human Participants of Koç University. The subjects washed their hands with commercial soap and rinsed with water before each measurement. Then, they dried their hands in the room temperature and ambient pressure. Also, the touch screen was cleaned by alcohol before each measurement.

Stimuli

We measured accelerations and forces under 48 different conditions; there were 2 waveforms (sinusoidal, square), 6 frequencies (15, 30, 60, 120, 240, 480 Hz), and 4

Table 3.2: Experimental Parameters.

Type	**Parameter**	**Value**	**Unit**
Test	**Frequency**	15, 30, 60, 120, 240, 480	Hz
	Waveform	Sinusoidal, Square	-
	Scan Speed	10, 20, 50, 100	mm/s
Control 1 (EMI Effect)	**Frequency**	15, 30, 60, 120, 240, 480	Hz
	Waveform	Sinusoidal, Square	-
Control 2 (No excitation)	**Scan Speed**	10, 20, 50, 100	mm/s

finger scan speeds (10, 20, 50, 100 mm/s), which are tabulated in Table 2. In each measurement, one parameter was changed while fixing the others. We selected the finger scan speeds based on the values used in the earlier studies [Fagiani and Barbieri, 2014b, Wiertlevski and Hayward, 2012, Yoshioka et al., 2007, Adams et al., 2013]. The amplitude of the input signals was chosen 8dB SL (sensation level: 8 dB higher than the threshold) more than the averaged threshold values measured in Experiment 1 (see Section 3.2.1).

Initially, we performed two separate control measurements to test the reliability of the collected data[4]. First, the forces and accelerations were measured when the finger was stationary in 12 conditions to observe the electromagnetic interference (EMI) effect on the sensors (Table 3.2). Second, the forces and accelerations were measured without any electrostatic excitation in 4 conditions (Table 3.2). Therefore, 64 different (48 test, 16 control) measurements were performed in total for each subject.

[4]In the first set of control measurements, we checked the signal to noise ratio (SNR). If the SNR value of a measurement was lower than 5 dB, that measurement was repeated. In the second set of control measurements, we checked the signal energies due to finger motion without any electrostatic excitation. These energies were compared to those obtained from the test measurements to investigate the effect of electrostatic excitation (see Section 3.3.2).

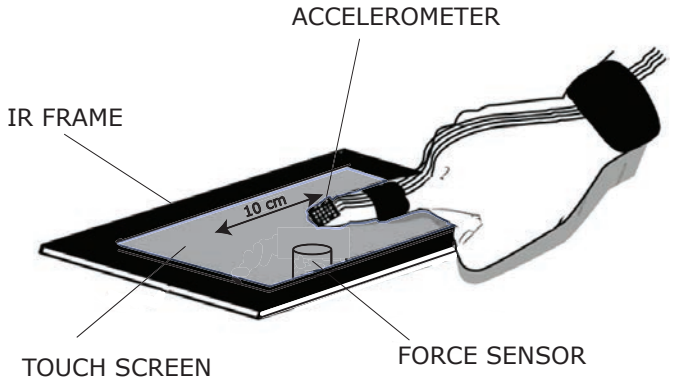

Figure 3.8: Illustration for the attachment of force sensor and accelerometer.

Experimental Setup

The experimental setup was similar to the one used in our psychophysical experiments (Fig. 3.6). For this experiment, the touch screen (SCT3250, 3M Inc.) was placed on top of a force sensor (Nano17, ATI Inc.). The sensor was attached to the screen and an aluminium base using double-sided adhesive tapes (3M Inc.). The aluminum base was also attached to a stationary table by the same adhesive tape. The touch screen was excited with a voltage signal generated by a signal generator (33220A, Agilent Technologies Inc.). The voltage signal from the generator was amplified by an amplifier (E-413, PI Inc.) before transmitted the touch screen. An IR frame was placed on top of the touch screen to measure the finger scan speed during experiments. An accelerometer (ADXL 335, Analog Devices Inc.) was glued on the fingernail of the subjects. The accelerometer and force data were acquired by two separate DAQ cards (USB-6251 and PCI-6025E, NI Inc.). The cables of the accelerometer were taped on the finger and arm of the subjects as shown in Fig. 3.8. Both accelerometer and force data were acquired using LabView (NI, Inc.). An arm rest was used to support the subjects' arm during the experiments. The subjects were asked to wear a ground strap on their stationary wrist. The subjects were also asked to synchronize their scan speeds with the speed of a visual cursor displayed on the computer screen.

Procedure

The subjects were instructed to sit on a chair in front of the experimental setup and move their index fingers back and forth in the horizontal direction on the touch screen. They were asked to move their finger only in a 10×3 cm rectangular region on the touch screen. They were asked to synchronize their fingers with the motion of a moving cursor on the computer screen. Also, they received visual feedback about the magnitude of the normal force that they applied to the touch screen. For this purpose, two led lights were displayed on the computer screen and used to keep the normal force between 0.1 and 0.6 N. We selected this range based on the normal forces reported in the literature as relevant to tactile exploration [Adams et al., 2013, Delhaye et al., 2014]. If the user applied less than 0.1 N to the touch screen, the led labelled as "press more" turned to green. However, if the user applied more than 0.6 N, the led labelled as "press less" turned to red. The subjects were instructed to complete four strokes (two forward, two backward) under each experimental condition.

Before starting the experiment, the subjects were given instructions about the experiment, and asked to complete a training session. This training session enabled subjects to adjust their finger scan speed and normal force before the actual experimentation. The experiments were performed in two blocks. The first and second blocks had six and seven sessions respectively. The experimental blocks were formed based on the input voltage waveform whereas the sessions were based on the input voltage frequency. The second block also contained one session without any input voltage. It took approximately 1.5 hours to complete all the measurements for a subject, including the time for attaching the accelerometer to the subjects' finger and the training session.

Data Analysis

The force and acceleration data were analyzed in Matlab. An example data collected during one session is shown in Fig. 3.9. The figure shows force and acceleration data recorded at different scan speeds. We calculated the displacement values by

integrating the acceleration data twice as suggested in [Gescheider et al., 2009].

The collected force, acceleration and displacement data were segmented according to the finger scan speed (see coloured regions in Fig. 3.9). Then, DC offset was removed from each segment by subtracting the mean values. To remove the low-frequency noise due to finger motion, data in each stroke was filtered by a high-pass filter having a cut-off frequency of 10 Hz. Afterwards, the RMS of each stroke was calculated and an average RMS was obtained for each finger speed using the data of 4 strokes.

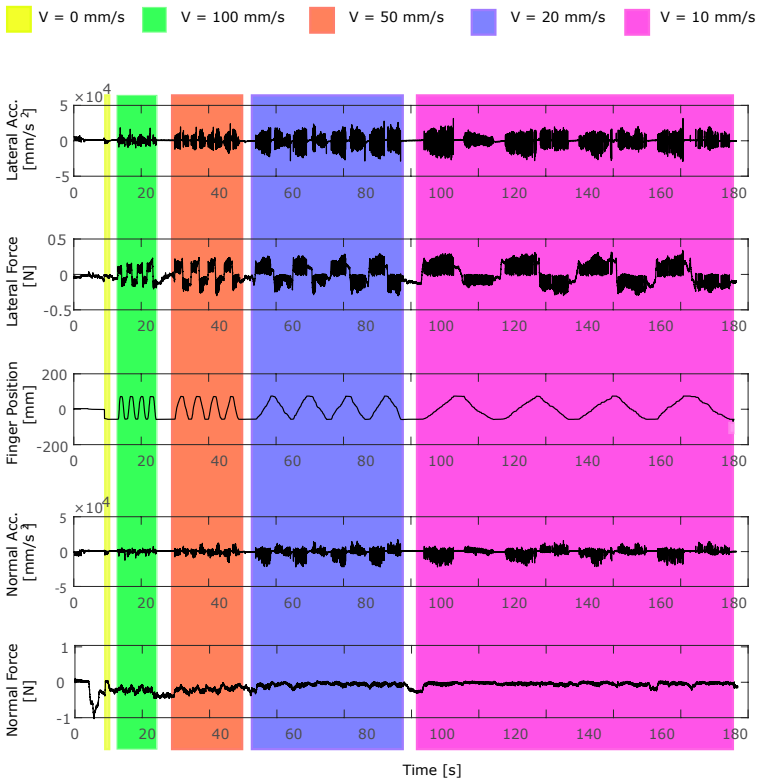

Figure 3.9: Data collected during one experimental session. The input voltage was a square wave at 60 Hz.

For detection analysis, power spectrum of each stroke was calculated for the signals in the normal direction. Then, an average power spectrum was obtained for each finger speed using the power spectrum of 4 strokes. The peak frequencies were determined using this spectrum. The energy (in unit time) of each peak frequency

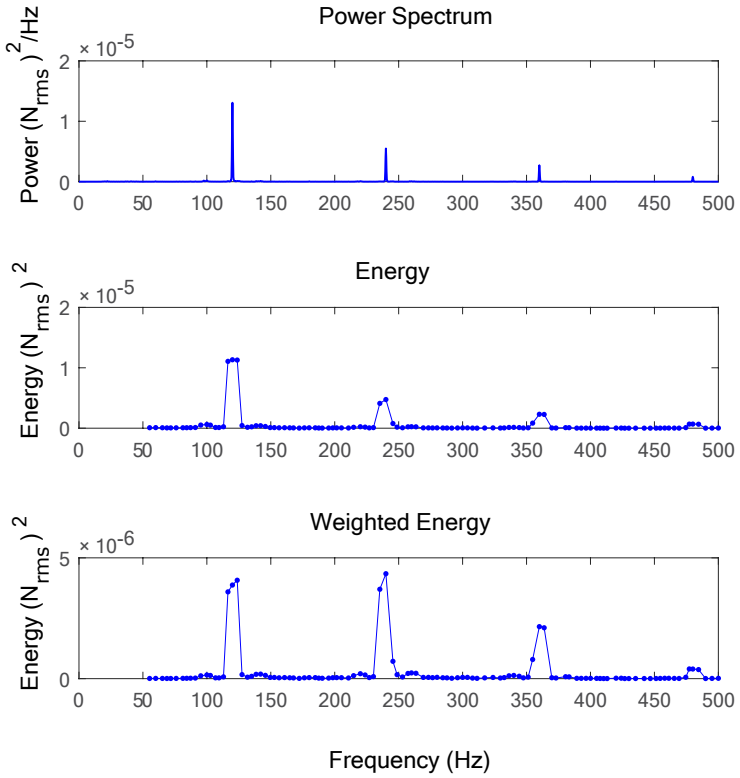

Figure 3.10: Exemplar plots of average power spectrum, energy (in unit time), and weighted energy as a function of frequency. The plots were generated using the force data recorded at the finger scan speed of 20 mm/s (the input voltage was a square wave at 60 Hz).

was calculated by integrating its power spectrum data for the peak interval. Finally, the calculated raw energies were multiplied by the inverse of the normalized human sensitivity function to obtain the weighted ones (Fig. 3.10). We used the human sensitivity functions reported in [Hatzfeld et al., 2016, Morioka and Griffin, 2005] for the force, acceleration and displacement data, respectively. Moreover, we calculated the corresponding electrostatic forces generated by the same waveforms and amplitudes via Matlab simulations. We also calculated the weighted energies of those simulated forces using the same data analysis approach discussed above.

In addition, the average friction coefficient was calculated by dividing the unfiltered lateral force of each stroke to those of normal force. Then, an average friction coefficient of each condition was obtained using the data of 4 strokes.

3.3 Results

3.3.1 Results of Experiment 1

Fig. 4.9 depicts the measured threshold voltages for seven fundamental frequencies (15, 30, 60, 120, 240, 480, 1920 Hz) and two different waveforms (sinusoidal and square).

We analyzed the results using two-way analysis of variance (ANOVA) with repeated measures. Both main effects (frequency and waveform) were statistically significant on the threshold levels ($p<0.01$). Moreover, there was a statistically significant interaction between frequency and waveform ($p<0.01$).

Additionally, the effect of the waveform on our tactile perception at each frequency was analyzed by Bonferroni corrected paired t-tests. The results showed that there was a statistically significant effect of the waveform on our haptic perception for fundamental frequencies less than 60 Hz. The difference between square and sinusoidal waves was significant at frequencies greater than and equal to 60 Hz. The corrected p-values for each frequency (15, 30, 60, 120, 240, 480, 1920 Hz) are 0.008, 0.016, 1, 1, 1, 0.168, and 0.128, respectively.

3.3.2 Results of Experiment 2

The RMS values calculated for each condition from acceleration and force data (lateral and normal), and friction coefficients are plotted against fundamental frequencies of the input signals (Fig. 3.12). The data from different scan speeds were averaged for the clarity of plots. The results were analysed using three-way analysis of variance (ANOVA) with repeated measures. The results showed that finger scan speed had a significant effect on force, acceleration, and friction coefficient ($p<0.05$).

To test the reliability of the measurement results, the average energies calculated for no electrostatic excitation were compared to those of electrostatic excitation using independent t-tests. Electrovibration generated a statistically significant difference in all calculated energies for both waveforms (sinusoidal and square) and for each

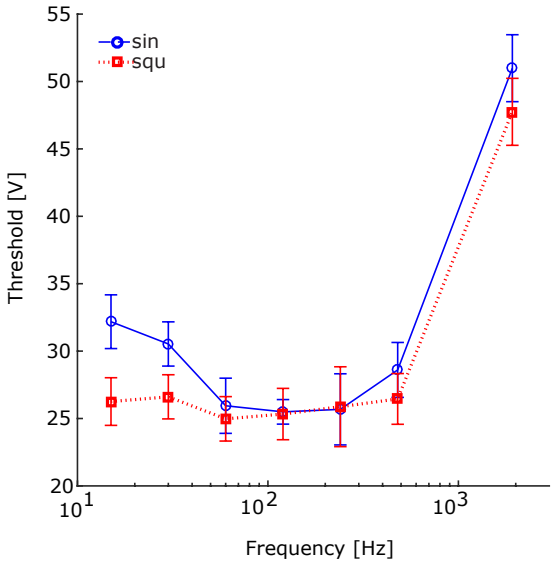

Figure 3.11: The average detection thresholds of the subjects for seven fundamental frequencies (15, 30, 60, 120, 240, 480, 1920 Hz) and two different waveforms (sinusoidal and square).

response type (acceleration, force, and displacement) ($p<0.05$).

The average weighted energies calculated for each actuated condition from displacement, acceleration and force data (normal) are plotted against fundamental frequencies of the input signal (Figs. 3.13a-c). They are also plotted as a function of the frequency component having the highest energy (Figs. 3.13e-g). The frequency interval in which the Pacinian channel is the most sensitive is marked as pink. Moreover, the average weighted energies estimated from Matlab simulations are also compared to those of the experimental results (Figs. 3.13d and h).

We analyzed the weighted energy results for all the measured variables using three-way analysis of variance (ANOVA) with repeated measures. The effects of waveform, frequency, and scan speed on the weighted energy were significant ($p<0.05$). Their interactions except the one between speed and frequency were also statistically significant ($p<0.05$). Moreover, Bonferroni corrected paired t-tests showed that the weighted energies were statistically different for sinusoidal and square waves at fundamental frequencies 15, 30 and 480 Hz ($p<0.05$), and similar for the other frequencies.

For square signals, we calculated the proportion of the frequency components that were within the sensitivity range of the Pacinian channel (100-500 Hz) to the total number of components for each response type (acceleration, force, and displacement) for measured and simulated variables. The results showed that the frequency components having the highest energies were accumulated between 100-500 Hz for the square signals.

3.4 Discussion

Our results showed that human perception of electrovibration on touch screens is frequency-dependent as in vibrotactile studies. The detection thresholds obtained from our psychophysical experiments (Fig. 4.9) followed the well known U-shaped human sensitivity curve. The threshold values were low between 60 Hz and 240 Hz, and higher for the rest. The corresponding detection energies of force (measured and simulated), acceleration (measured) and displacement (measured) signals calculated at these thresholds naturally displayed an inverted U-shape trend as a function of frequency (Figs. 3.13a-d). These results are consistent with the existing vibrotactile literature [Güçlü and Öztek, 2007, Yıldız and Güçlü, 2013, Gescheider et al., 2002, Bolanowski et al., 1988, Morioka and Griffin, 2005]. In earlier studies, the detection thresholds of the index or middle finger were measured as a function of frequency by using various contactors. Typically, sinusoidal displacements with slow onset and offset times was used as stimuli, which generate mechanical excitation with a single frequency component. In our case, alternating electrostatic forces are generated at the contact interface based on the square of the voltage applied to the touch screen (Equation 2.2). This nonlinear transformation introduces frequency components not present in the original signal. For example, when a pure sinusoidal voltage is applied to the touch screen, the force waveform has twice the frequency of the input wave. Hence, the detection results presented in Fig. 4.9 for square and sinusoidal stimuli should be interpreted by multiplying the values on the frequency axis with a factor of two. When the calculated energies are plotted against the frequency component

having the highest energy (Fig. 3.13 e-h), the peak values are between 100 and 500 Hz, which is similar to those reported in the earlier vibrotactile literature [Gescheider et al., 2002, Morioka and Griffin, 2005, Güçlü and Öztek, 2007]. [Bau et al., 2010] measured absolute detection thresholds of electrovibration stimuli for sinusoidal inputs. Their results also followed a U-shaped trend, but their detection threshold values for sinusoidal inputs were slightly lower than our results. This difference might be caused by the experimental factors such as the angle of contact, movement direction, environmental factors such as finger moisture and contact temperature, the number of subjects, and subject-to-subject variability such as the variability in fingerprints and finger electromechanical properties [Pasumarty et al., 2011, Derler and Gerhardt, 2012, Delhaye et al., 2014, Andre et al., 2011, Derler et al., 2009, Adams et al., 2013].

We found that participants were more sensitive to square excitation than sinusoidal one for frequencies lower than 60 Hz. The results suggested that Pacinian channel was the primary psychophysical channel in the detection of the electrovibration stimuli caused by all the square-wave inputs tested in this study. If a complex waveform, i.e. one which has many frequency components, is applied to the touch screen, the frequency components in the range of 50-250 Hz would be mostly active in stimuli detection due to the high sensitivity of Pacinian channel at twice of these frequencies. For example, due to electrical filtering of finger, low-frequency components of a square wave excitation are suppressed. Therefore, the voltage across the dielectric layer contains exponentially decaying high-frequency transients. The electrostatic force generated based on these transients is rather complex, including twice the frequencies and distortion products of the input signal components. Due to the frequency-dependent human tactile sensitivity, the frequency components in the force waveform will not be equally effective in detection (see Fig. 3.5). For example, when the weighted energies are plotted as a function of fundamental frequencies (Fig. 3.13 a-d), it is difficult to interpret the results in terms of tactile detection. On the other hand, when the weighted energies are plotted as a function of frequency components

with the highest energies in the force, acceleration, and displacement signals in our study (Fig. 3.13 e-h), the peak values fell into the range of 100-500 Hz (see the pink regions in Fig. 3.13 e-h), which suggest that mainly the Pacinian channel was effective in detection for square wave inputs [Bolanowski et al., 1988, Gescheider et al., 2002].

In Matlab simulations, we used the values of the human skin parameters (ρ_{sc} and ϵ_{sc}) measured at the *fundamental* frequencies. Although this is a valid assumption for the sinusoidal wave, it is a simplification for the square wave, since square wave contains many frequency components. This limitation might have contributed to the differences in experimental and the simulation results. In general the force amplitudes and energies estimated through simulations were lower than those measured through experiments for both square and sinusoidal waves (Fig. 3.13 d, h). Experimental factors such as moisture, temperature, and subject-to-subject variability of fingertip mechanical and electrical properties might have contributed to the differences [Pasumarty et al., 2011, Derler and Gerhardt, 2012, Delhaye et al., 2014, Andre et al., 2011, Derler et al., 2009, Adams et al., 2013]. For example, measuring electrical impedances directly from the subjects might lead to a better match of the experimental and simulation results. Also, future models of mechanical interpretation of electrovibration may help to explain the mismatch. For example, a more accurate estimation of the force energies at the mechanoreceptor level could potentially be obtained by linking the electrostatic forces generated at the fingerpad to the mechanical forces measured at the contact interface during finger movement.

The changes in RMS of measured mechanical forces, accelerations and friction coefficients as a function of waveform were not significant most probably because the input signals were normalized referenced to the threshold levels. However, when we inspect Fig. 3.12, the RMS values as a function of frequency are almost constant. This has to be due to the nature of RMS measurement which is not suitable for modelling the detection. On the other hand, it simplifies the illustration of time varying sensor output data.

Measured force, acceleration and friction coefficients were affected by finger scan

speed in a complex manner suggesting that it might also affect our haptic perception accordingly. The results showed that the magnitude of contact forces and accelerations were appeared to be positively correlated with the scan speed though the friction showed a negative correlation. Similar results were also obtained in the earlier studies. Using an artificial finger which had similar electrical and mechanical properties of a real human finger, [Mullenbach et al., 2017] investigated that lateral forces generated by electrovibration increased as a function of scan speed. Moreover, in our experiments the acceleration and force energies increased as the scan speed was increased. The earlier studies in tribology literature support this result [Tang et al., 2015, Fagiani and Barbieri, 2014a, Fagiani et al., 2011, Pasumarty et al., 2011, Bensmaia and Hollins, 2011]. The effect of scan speed on the measured forces and accelerations and their energies suggest that the viscoelastic characteristics of human finger also plays a role in tactile sensing of electrovibration. The possible effect of skin mechanics on psychophysical detection thresholds were also suggested by [Yıldız and Güçlü, 2013]. In that study, they measured vibrotactile detection thresholds of Pacinian channel at 250 Hz and mechanical impedances of fingertips of seven subjects. They reported that there was a significant positive correlation between loss moduli of the skin and detection thresholds.

As far as we know, this is the first study which investigates the effect of input voltage waveform on haptic perception of electrovibration in the frequency domain. The earlier research studies have already investigated the detectability and discriminability of mechanical waveforms in real and virtual environments and the results of these studies can be compared with ours. For example, [Summers et al., 1997], observed that vibrotactile sine waves and monophasic/tetra-phasic pulses at suprathreshold levels resulted in similar scores in a frequency identification task. They concluded that temporal cues are more important than spatial cues in that particular task. We think their results can be interpreted that the strongest frequency component in complex waveforms (after correction for human sensitivity) drives the stimulus detection. [Cholewiak et al., 2010] investigated the perception of virtual gratings containing mul-

tiple spectral components. They performed detection and discrimination experiments with virtual sinusoidal and square gratings displayed by a force-feedback device at various spatial frequencies. Their results showed that detection thresholds of square gratings were lower than the sinusoidal ones at lower spatial frequencies. Similar to our results, they explained that the square gratings are detected based on their harmonic components having the lowest detection threshold.

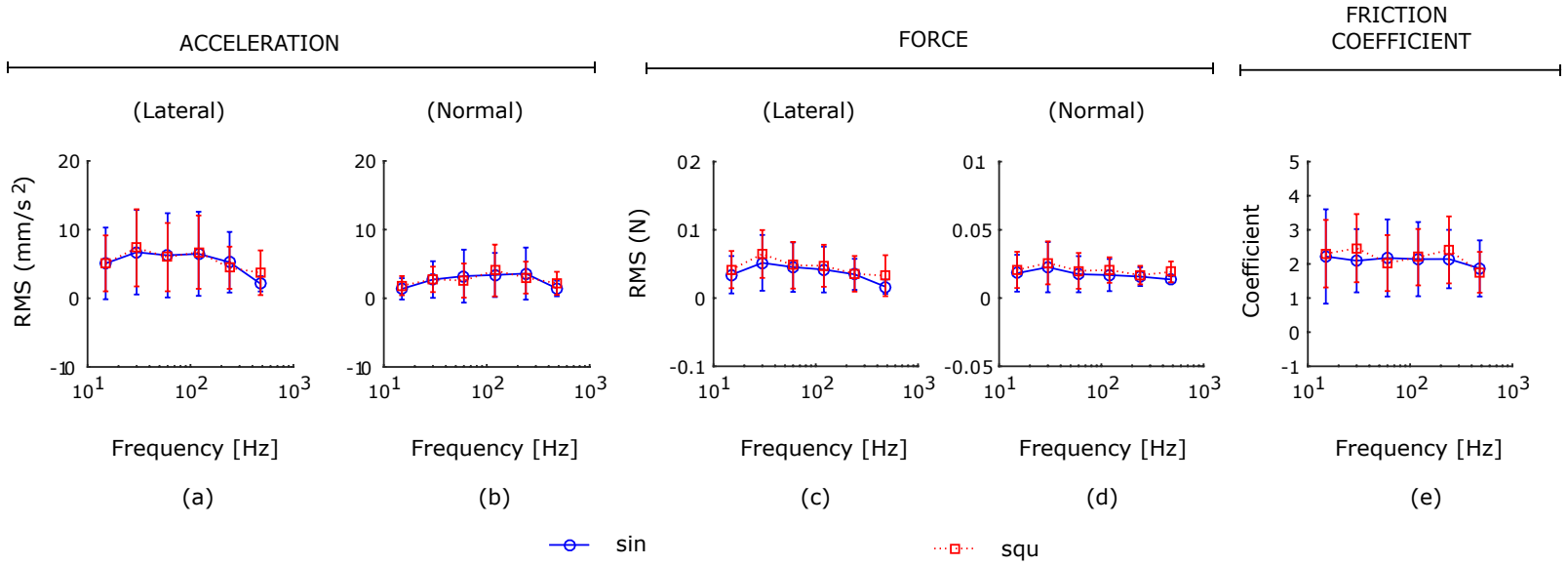

Figure 3.12: The means and standard deviations of acceleration (a-b), force (c-d), and friction coefficient (e). The data from different scan speeds were averaged for the clarity of plots.

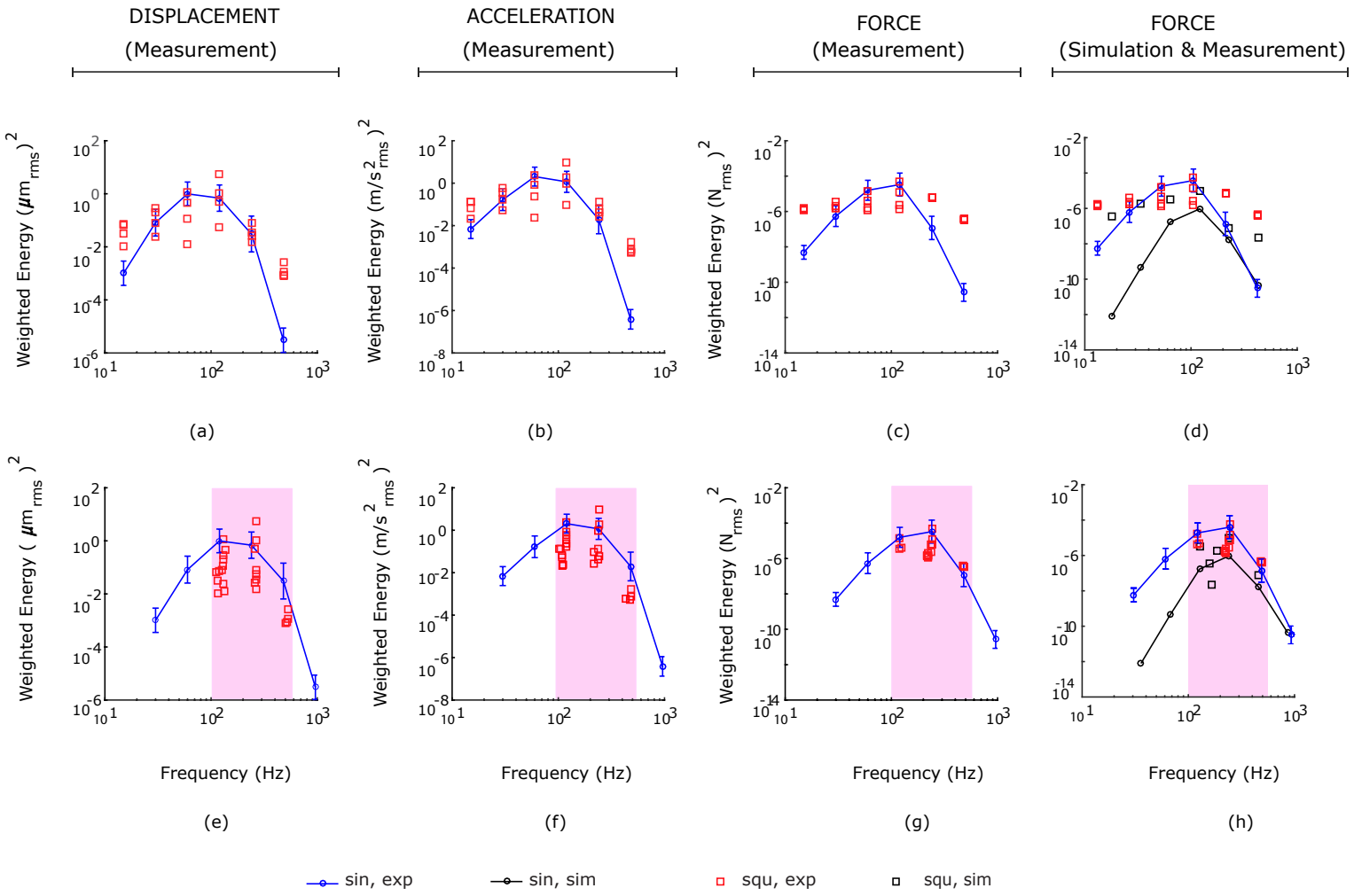

Figure 3.13: The weighted energies of the displacement, acceleration, and force signals at threshold are plotted against the input fundamental frequency (a-c) and the frequency component with the highest energy (e-g). The output data for the input sinusoidal signals recorded at different scan speeds were averaged for the clarity of plots. The output data for the input square signals were not averaged because they contain energy components at many frequencies. The weighted energies of the simulated force signals at threshold are plotted against the fundamental frequency (d) and the frequency component with the highest energy (h) and compared with those of the measurements. The pink regions indicate the frequency interval where the Pacinian channel is the most sensitive.

Chapter 4

EFFECT OF MASKING ON TACTILE PERCEPTION BY ELECTROVIBRATION

Summary

In this chapter[1], we investigate the effect of masking on the tactile perception of electrovibration displayed on touch screens. Through conducting psychophysical experiments with nine subjects, we measured the masked thresholds of sinusoidal electrovibration bursts (125 Hz) under two masking conditions: simultaneous and pedestal. The masking stimuli were noise bursts, applied at five different sensation levels varying from 2 to 22 dB SL, also presented by electrovibration. For each subject, the detection thresholds were elevated as linear functions of masking levels for both masking types. We observed that the masking effectiveness was larger with pedestal masking than simultaneous masking. Moreover, in order to investigate the effect of tactile masking on our haptic perception of edge sharpness, we compared the perceived sharpness of edges separating two textured regions displayed with and without various masking stimuli. Our results suggest that sharpness perception depends on the local contrast between background and foreground stimuli, which varies as a function of masking amplitude and activation levels of frequency-dependent psychophysical channels.

4.1 Materials and Methods

4.1.1 Participants

We conducted experiments with nine (three female and six male) subjects having an average age of 26 (SD: 3). Except for one male subject (S2), all of the subjects were

[1]This chapter is based on an article [Vardar et al., 2017b].

right-handed. The subjects read and signed the consent form before the experiments. The form was approved by Ethical Committee for Human Participants of Koç University. Before each measurement, the subjects washed their hands with commercial soap and rinsed with water. Then, they dried their hands in the room temperature. Also, the touchscreen was cleaned by alcohol before each measurement.

4.1.2 Apparatus

A touchscreen (SCT3250, 3M Inc.) was placed on top of a force sensor (Nano17, ATI Inc.). The sensor was attached to the screen and a plexiglass base using double-sided adhesive tapes (3M Inc.). The plexiglass base was also attached to an LCD screen (Philips Inc.) by the same adhesive tape. The touchscreen was excited with a voltage signal generated by a DAQ card (USB-6051, NI Inc.) and further amplified (PZD700A, TREK Inc.). The force data was acquired by another DAQ card (PCI-6025E, NI Inc.). An IR frame was placed on top of the touch screen to measure the finger scan speed during experiments (see Fig. 4.1). The subjects were asked to synchronize their scan speeds with the motion of a visual cursor displayed on the LCD screen. Subjects entered their responses through a keyboard. They were asked to put on an anti-static strap on their stationary wrist for grounding. For isolation of the background noises, subjects were asked to wear headphones displaying white noise during experiments.

4.1.3 Stimuli

Threshold & Masking Experiments

The input voltage signals were bursts of sinusoidal, noise or combination of both depending on the experiment (see Table 3.2). All signals started and ended as cosine-squared ramps with 50 ms rise and fall times. This method enables smooth stimulation of the skin with the desired frequency [Makous et al., 1995a, Güçlü and Öztek, 2007]. The duration of the test stimuli was 0.5 s as measured between half-power points of the bursts. Duration of the masking stimuli were 0.5 and 2 s for simultaneous and

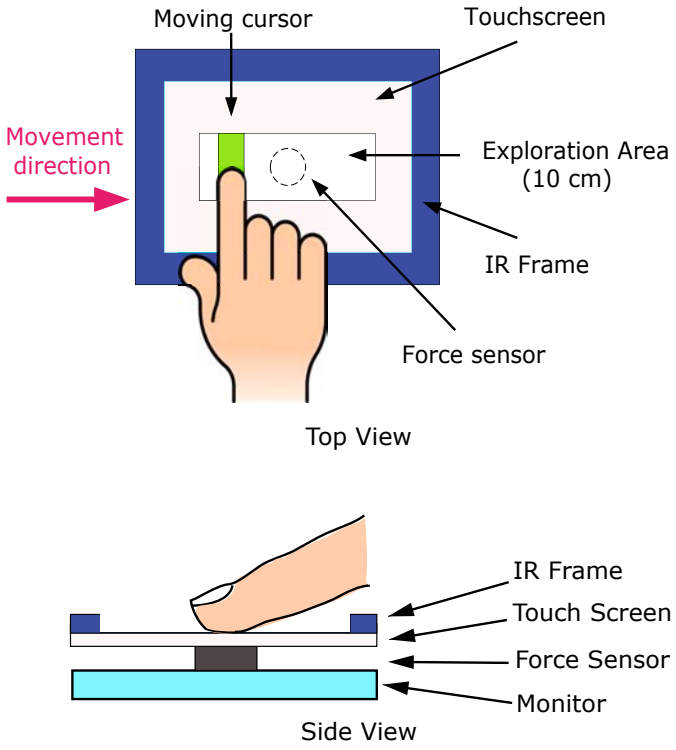

Figure 4.1: Illustration of the apparatus used in experiments.

pedestal masking experiments respectively (see Fig. 4.2).

In detection threshold experiments, 125 Hz sinusoidal waveform and narrow band-limited noise (NBN) were used as test signals. The noise signals were generated by passing the output of a Gaussian white noise through a band-pass filter having a bandwidth of 75-200 Hz. This bandwidth range sets the upper and lower frequency limits as 1.6 times of the center frequency (125 Hz). Both sinusoidal and noise signals were chosen carefully to stimulate Pacinian channel. In Chapter 3, we showed that the detection of electrovibration stimuli depends on both electrical properties of human skin, electrostatic force generation due to capacitance coupling, and human psychophysical sensitivity. The resultant electrostatic force should be analyzed in frequency domain to determine the highest frequency components which would mediate detection. For example, because of the non-linearity in the physical formula in Equation 2.2, 125 Hz sinusoidal excitation results in electrostatic force at 250 Hz.

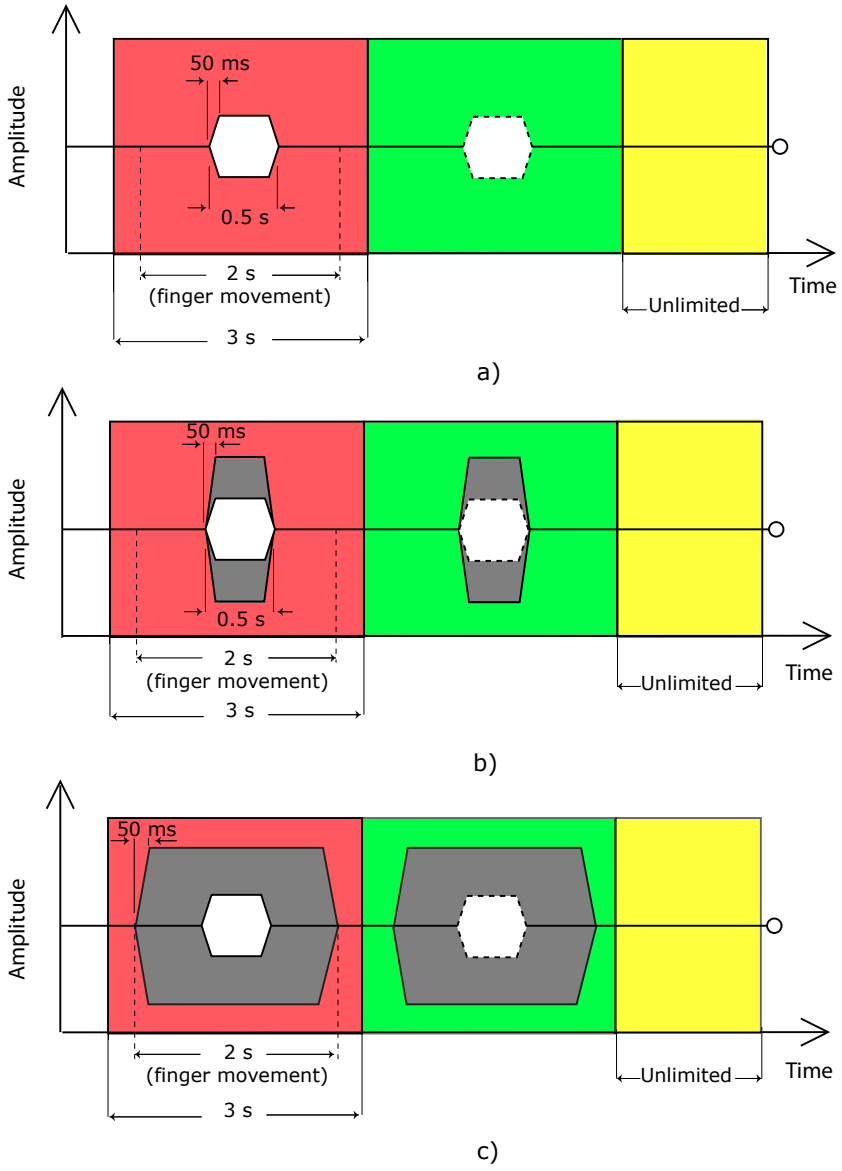

Figure 4.2: Stimulus timing diagrams for threshold and masking experiments. The stimuli were generated by bursts of input voltage signals applied to the touchscreen and displayed in two temporal intervals, which were signalled to subjects as red and green. In each interval, subjects explored the touch screen in one stroke with a scan speed of 50 mm/s. Each stroke lasted for 2 seconds. The subjects gave their responses in a third interval displayed as yellow. a. In absolute detection threshold experiments, the stimulus was displayed in either red or green interval randomly. b. In simultaneous masking experiments, the masking stimulus (gray) was displayed in both red and green intervals, but the test stimulus (white) was displayed randomly in only one interval. c. In pedestal masking experiments, the masking stimulus was longer (2 seconds) and displayed in both intervals. The test stimulus was displayed randomly in only one interval.

Table 4.1: The stimuli used in the threshold and masking experiments.

Experiment	**Test Stimuli**	**Test Duration**	**Masking Stimuli**	**Masking Duration**	**Masking Level**
Detection Threshold	125 Hz sinusoidal, NBN (75-200 Hz)	0.5 sec 0.5 sec	-	-	-
Simultaneous Masking	125 Hz sinusoidal	0.5 sec	NBN (75-200 Hz)	0.5 sec	5-22 dB SL
Pedestal Masking	125 Hz sinusoidal	0.5 sec	NBN (75-200 Hz)	2 sec	2-20 dB SL

For preparing the electrovibration stimuli in this study we used the model in Chapter 3, and analyzed the electrostatic forces in frequency domain after weighting with the human sensitivity curve. The frequency of the spectral components with highest energies were around 200-300 Hz (see Fig. 4.3). This is the frequency range where Pacinian channel is the most sensitive [Bolanowski et al., 1988, Gescheider et al., 2002, Güçlü and Öztek, 2007].

In masking experiments, the test signal was sinusoidal wave with a frequency of 125 Hz, whereas the masking signal was the noise burst used in the detection experiments. The masking and test voltage signals were summed before actuating the touch screen. The masking signal amplitudes were determined based on the RMS of the measured detection thresholds of the noise signals. The masking stimulus levels were expressed in dB above this threshold (i.e. sensation level, SL). We used masking stimuli at five different sensation levels (2-22 dB SL). Therefore, these levels were based on each subjects' individual psychophysical sensitivity.

Sharpness Experiments

The edges were displayed as short bursts (100 ms) of 125 Hz sinusoidal waves with an amplitude of 20 dB SL (see Fig. 4.4). The masking signals were similar to the ones used in Experiment 1 (see Table 4.2). They were band-limited noise signals

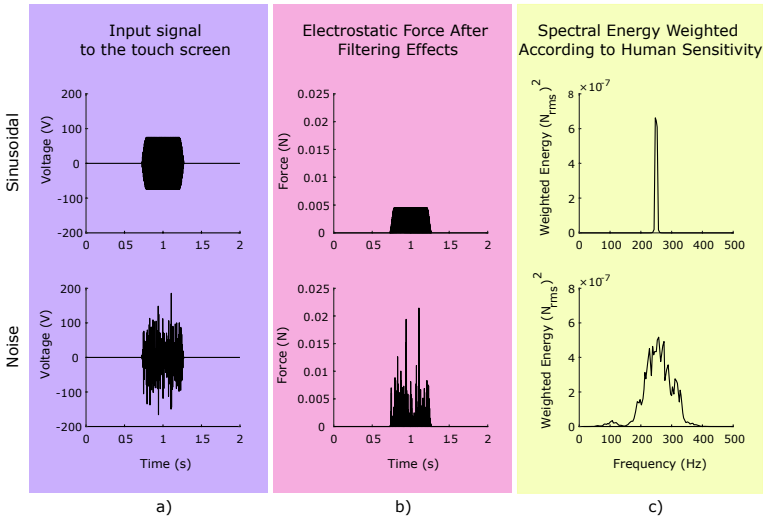

Figure 4.3: a. Exemplar sinusoidal and noise signals used in the absolute detection threshold experiments. Here, both signals have equal RMS amplitudes (50 V). b. The electrostatic forces were estimated using the simulation model in Chapter 3. The spectral energies were weighted according to human sensitivity curve in Chapter 3. c. For both sinusoidal and noise signals, the spectral components with highest energies were between 200-300 Hz.

with durations of 0.1 s (simultaneous) and 2 s (pedestal). Their RMS amplitudes were selected as 5, 10, and 15 dB SL. Both edge and background signals were started and ended as cosine-squared ramps with 20 ms rise and fall times (see Fig. 4.4a, b). We also used a low-frequency background noise (selectively chosen) to activate the NPI channel. The amplitude of this signal was 15 dB over the detection level of the high frequency noise signal found in initial experiments. This way, we were able to investigate the effect of noise band frequency on sharpness perception by keeping the excitation amplitude relatively constant based on detection level. Additionally, we used a ramped signal as a masking background to investigate the influence of local effects. Fig. 4.4c shows the timing specifications of this background signal. The RMS of the ramped signal was 15 dB SL. To illustrate the stimuli used in the sharpness experiments, we rendered gray scale images based on the electrostatic force outputs of our model [Vardar et al., 2017a] for the applied input voltage signals (see Fig. 4.5). We normalized the logarithmic values of the electrostatic force to vary between 0 and

Table 4.2: The stimuli used in the sharpness experiments.

Names	**Stimuli**	**Duration**	**Level**
E (Simple Edge)	125 Hz sinusoidal	0.1 s	20 dB SL
PM1 (Pedestal Masking 1)	NBN (75-200 Hz)	2 s	5 dB SL
PM2 (Pedestal Masking 2)		2 s	10 dB SL
PM3 (Pedestal Masking 3)		2 s	15 dB SL
SM1 (Simultaneous Masking 1)		0.1 s	5 dB SL
SM2 (Simultaneous Masking 2)		0.1 s	10 dB SL
SM3 (Simultaneous Masking 3)		0.1 s	15 dB SL
R (Ramped Pedestal Masking)		1.68 s	15 dB SL
PML (Pedestal Masking Low Frequency)	NBN (10-20 Hz)	2 s	Equal to PM3

1, where zero represented lowest intensity (black), and 1 represented highest intensity (white).

4.1.4 Procedure

We used two-alternative-forced-choice method in our experiments [Güçlü and Öztek, 2007]. The stimuli were displayed in two temporal intervals, which were signalled to subjects as red and green using a graphical user interface (GUI) designed in Matlab. Each interval lasted for three seconds. Subjects were instructed to hold their finger at an initial point when the red signal appeared on the screen. Subjects' were asked to move their fingers in tangential direction while synchronizing their finger movements with the motion of a moving cursor for two seconds. The speed of the cursor was 50 mm/s. When they finished one stroke, they were asked to raise their finger and bring it back to the initial point. Then, they repeated the same procedure for the green interval. After the green interval ended, a third interval (yellow) was started, where subjects were asked to make their choices as RED or GREEN.

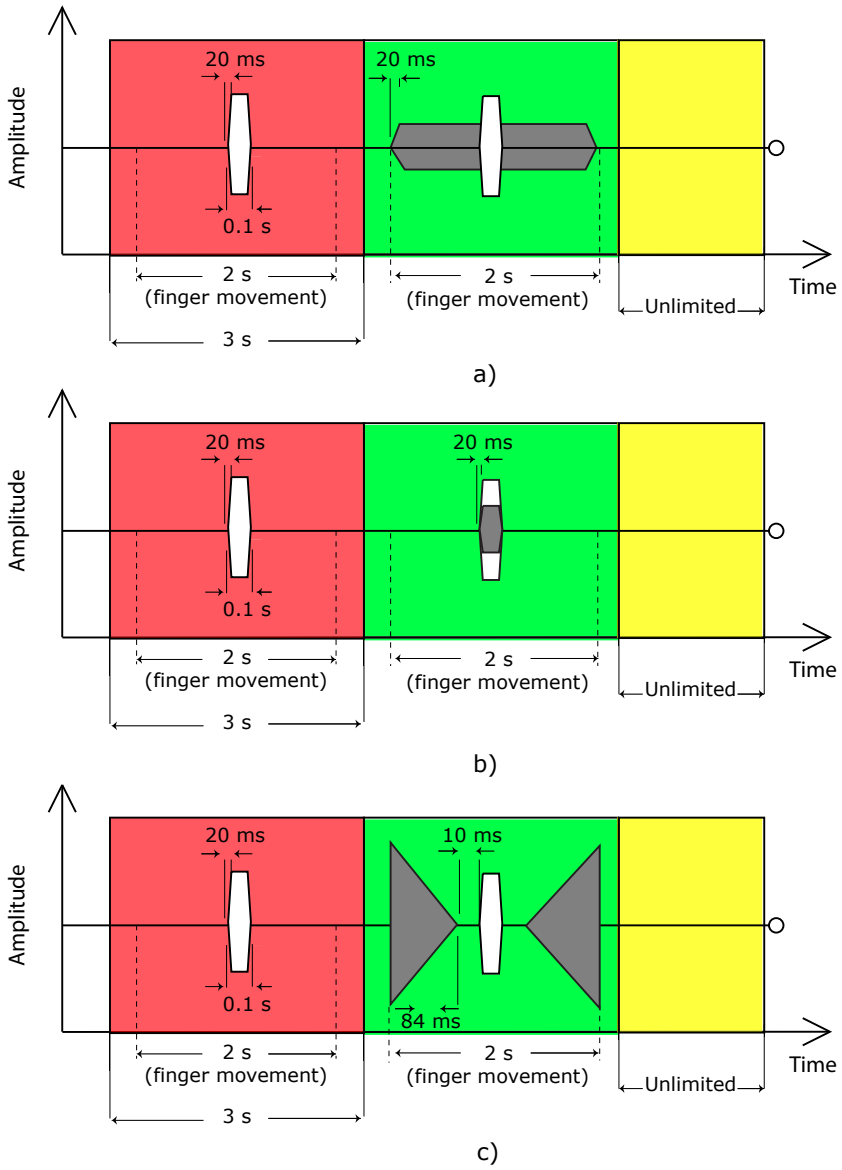

Figure 4.4: Stimulus timing diagrams for sharpness experiments. The test stimuli (white) are perceived as edges during finger scanning. The stimuli were displayed in two temporal intervals, which were signalled to subjects as red and green. In each interval, subjects explored the touch screen in one stroke with a scan speed of 50 mm/s. Each stroke lasted for 2 seconds. They gave their responses in a third interval displayed as yellow. An edge with no masking was compared to edges displayed with a. pedestal masking (gray), b. simultaneous masking (gray), and c. ramped pedestal masking (gray).

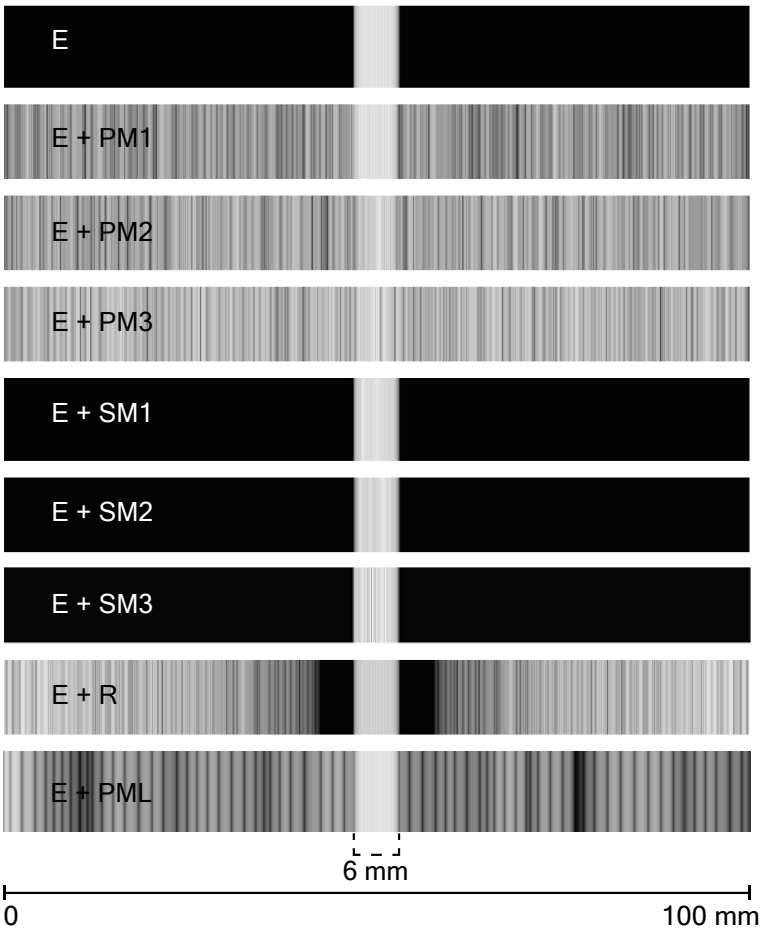

Figure 4.5: The gray scale images rendered depending on the electrostatic force outputs of our model (Chapter 3) in sharpness experiments. The logarithmic values of electrostatic force were normalized between 0 and 1, where zero represents lowest intensity (black), and 1 represents highest intensity (white).

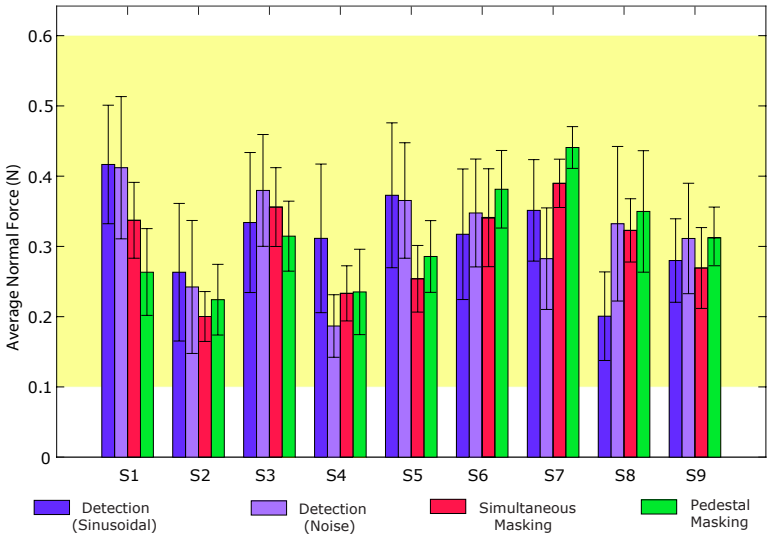

Figure 4.6: The average normal force applied by each subject during threshold and masking experiments and their standard deviations (excluding out of range values). The average normal force for all subjects was 0.31 N (SD: 0.06). For out of range measurements, the trial was repeated. The desired normal force range is marked as the yellow area.

Threshold & Masking Experiments

In these experiments, the task was to decide whether the test stimulus was in the red or the green interval. The location of the test stimulus was randomized in each trial. In each trial, average normal force and scan speed were also recorded. If the normal force and or scan speed of a subject were not in the desired range (0.1-0.6 N, and $\pm$ 25% of 50 mm/s), the trial was repeated until a measurement within the range was obtained. The psychophysical data came from within the range trials. We selected this range based on the normal forces and speeds reported in the literature as relevant to tactile exploration [Adams et al., 2013, Yıldız et al., 2015]. Figs. 4.6 and 4.7 show the average normal force and scan speed measured for each subject in different experiments (excluding out of range readings).

We changed the amplitude of the test signal, using three-up/one-down adaptive staircase method. This procedure estimates thresholds with 75 % correct probability of detection [Zwislocki and Relkin, 2001]. Each session was started by an initial

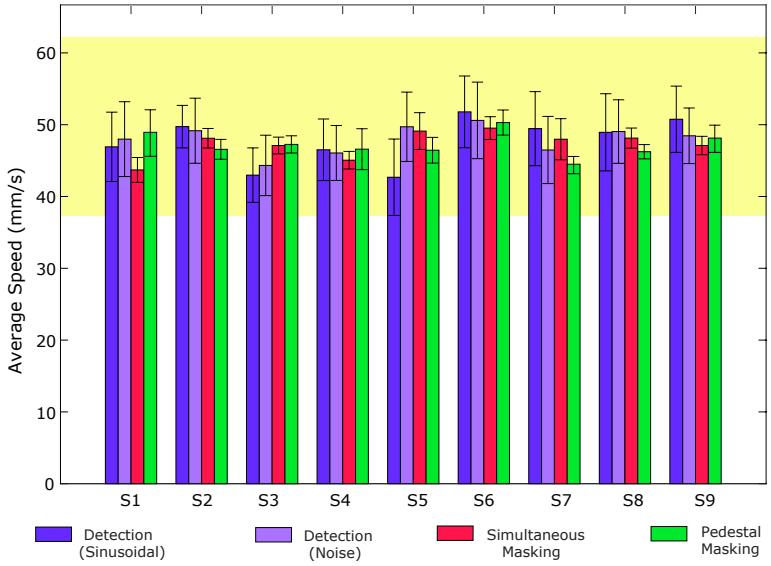

Figure 4.7: The average speed of each subject measured during in threshold and masking experiments and their standard deviations (excluding out of range values). The average speed for all subjects was 47.6 mm/s (SD: 2.2). For out of range measurements, the trial was repeated. The desired speed range is marked as the yellow area.

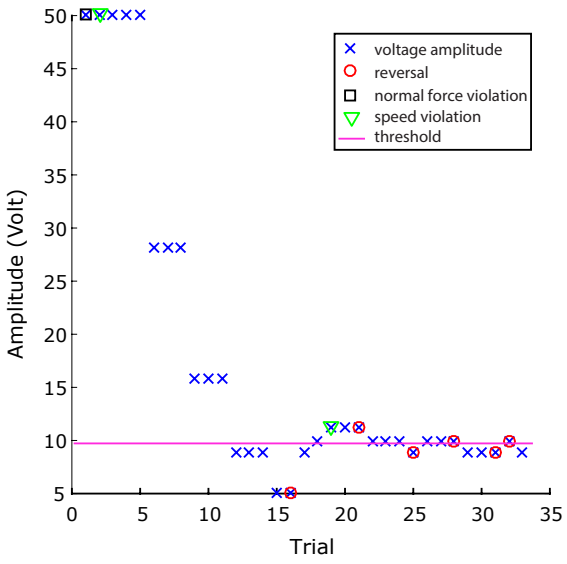

Figure 4.8: An exemplar staircase obtained from the detection threshold experiments. The amplitude of the stimulus was changed adaptively based on the three-up/one-down staircase method [Zwislocki and Relkin, 2001]. The step size was 5dB until the first reversal, then it was decreased to 1 dB. The trials in which subject violated the normal force and speed constraints were repeated. The threshold was calculated as the average of the last five reversals at ± 1dB range.

voltage with sufficiently high amplitude. If the subject gave three correct responses (not necessarily consecutive), the voltage level was decreased by 5 dB. If the subject gave one incorrect response, the voltage level was increased by 5 dB. The change of the response from correct to incorrect or the vice versa was counted as one reversal. After one reversal, the step size was decreased to 1 dB. The experiments were stopped automatically if the reversal count was five at the ± 1 dB level (see Fig. 4.8). The threshold was calculated as the mean of the last five reversals. In one session, approximately 35-60 trials were presented until reaching the threshold.

Before starting the experiments, the subjects were given instructions and asked to complete a training session. This training session enabled subjects to adjust their finger scan speed and normal force before the actual experimentation. Each subject completed the experiments in 24 sessions (2 signal types $\times$ 2 repetitions for threshold experiments, and 5 masking levels $\times$ 2 masking types $\times$ 2 repetitions for masking experiments), executed in separate days. The duration of each session was about 15-20 minutes.

Sharpness Experiments

In these experiments, the task was to choose the interval in which they perceived the edge sharper. In each trial, a simple edge with no masking (a sinusoidal burst without any background noise) was compared to an edge with a masking stimulus. There were eight different masking stimuli displayed in random order. The location of interval for sharper edge was also randomized in each trial. Before the experiments, the subjects were given instructions and asked to complete a training session. The subjects completed the sharpness experiments in two sessions, executed in separate days. In total, each stimuli pair was displayed for twelve times (six times in each session). The duration of each session was about 15 minutes.

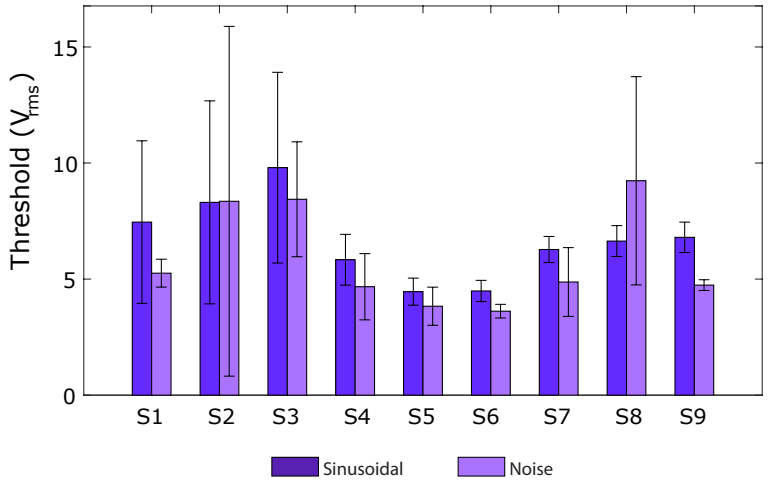

Figure 4.9: Absolute detection thresholds measured for sinusoidal (125 Hz) and noise (NBN) test signals of nine subjects. The error bars indicate the standard deviations.

4.2 Results

4.2.1 Results of Threshold Experiments

The detection thresholds measured for sinusoidal and noise (NBN) test signals of nine subjects are shown in Fig. 4.9. Paired t-test shows that there was no significant difference between the detection thresholds of sinusoidal (M: 6.67, SD: 1.71) and noise (M: 5.89, SD: 2.16) stimuli (p-value = 0.143), since the peak energies of their frequency components were equalized before the experiments, as explained in Section 4.1. The detection energies and frequencies of both test signals were investigated for each measured threshold using the model in Chapter 3. Paired t-test indicates that there was no significant difference between the detection energies of sinusoidal (M: 1.93e-10, SD: 3.51e-10) and noise (M: 4.73e-11, SD: 6.8e-11) stimuli (p-value = 0.241). Moreover, there was no significant difference between detection frequencies of sinusoidal (M: 250, SD: 0) and noise (M: 254.7, SD: 5.82) stimuli (p-value = 0.08). This further verifies that the test signals were detected by the Pacinian psychophysical channel (see Fig. 4.10).

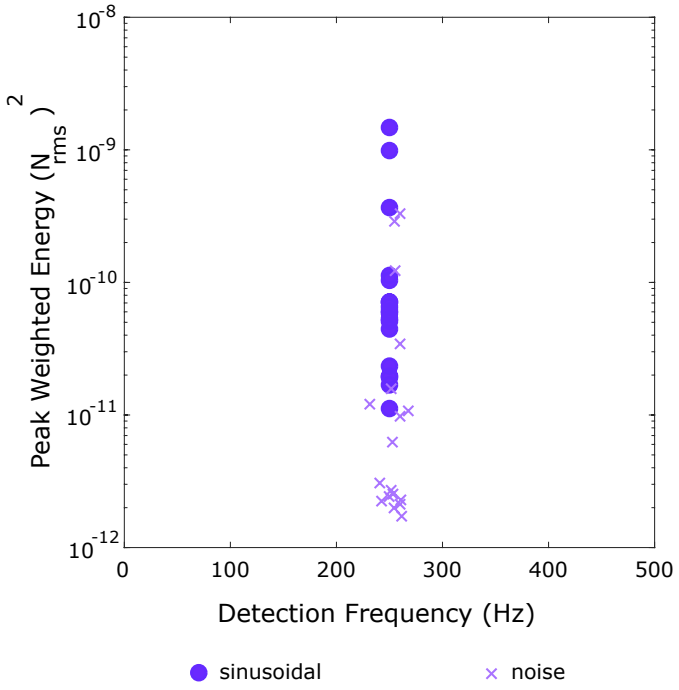

Figure 4.10: Frequencies and energies of highest spectral components at threshold levels. Spectral components were calculated using the model in Chapter 3. Note that, this model estimates resultant electrostatic forces based on a circuit model without including mechanical effects. The input to the model was determined according to each psychophysical threshold measurement. The measured force data was not presented due to the limited sensitivity range of the sensor.

4.2.2 Results of Masking Experiments

The detection thresholds (test signal: 125 Hz sinusoidal) of each subject were elevated by both simultaneous and pedestal masking. The threshold shifts were plotted as a function of masking level in dB SL for each subject (Fig.4.11). Pearson correlation coefficients were computed to assess the relationship between the threshold shifts and masking levels. There was a strong positive and significant correlation between them for both masking types (see Table 4.3). A linear regression model was used to predict threshold shift based on masking level (Table 4.4). As can be seen in the regression plots, the threshold shifts were linear and had slopes close to 1. When the data was plotted based on subject averages (Fig. 4.12), and the analyses were repeated, the correlation coefficients were 0.994 and 0.973 for simultaneous and pedestal masking

Table 4.3: Pearson coefficients for the correlation between threshold shift and masking level. ** Correlation is significant at 0.01 level. * Correlation is significant at 0.05 level.

Subjects	**Pearson Coefficient (r)**	
	Simultaneous	**Pedestal**
S1	0.985**	0.992**
S2	0.971**	0.949*
S3	0.997**	0.924*
S4	0.994**	0.995**
S5	0.975**	0.964**
S6	0.985**	0.972**
S7	0.989**	0.990**
S8	0.980**	0.955*
S9	0.993**	0.983**
All	0.994**	0.973**

respectively (All in Table 4.3). The threshold shifts were usually higher with pedestal masking compared to simultaneous masking (Fig. 4.11). When the subject averages were analyzed, the intercept of the threshold shift was 1.549 and 0.378 for pedestal and simultaneous masking respectively (All in Table 4.4). Furthermore, pedestal masking caused a higher increase in threshold shift as characterized by the slopes calculated for subject averages (0.967 vs 0.884). We also analyzed the effect of masking type and level on the resultant threshold shifts by using a linear mixed effect model with random intercept and slope [Landau and Everitt, 2004]. As seen in Table 4.5, the effects of masking type and level were significant (p-values <0.01). However, in this model, we assumed there was no interaction between those two factors, since the red and green lines in Fig. 4.12 have approximately similar slopes (Table 4.4).

Table 4.4: Results of the linear regression analysis. A linear model in the form of (y = mx+n) was fitted to the experimental data of threshold shift versus masking level. ** Regression is significant at 0.01 level. *Regression is significant at 0.05 level.

	Value	**S1**	**S2**	**S3**	**S4**	**S5**	**S6**	**S7**	**S8**	**S9**	**All**
Simultaneous	**m**	1.041	1.137	0.867	1.227	1.137	1.147	0.849	1.053	1.397	0.884
	n	-7.057	-1.14	1.867	-5.48	-6.243	-4.29	2.693	0.746	-10.38	0.378
	$\mathbf{R^2}$	0.971**	0.943**	0.994**	0.987**	0.950**	0.970**	0.977**	0.960**	0.986**	0.988**
Pedestal	**m**	1.163	0.876	0.861	1.606	1.444	1.374	1.46	1.084	1.34	0.967
	n	-1.384	2.957	4.516	-5.027	-5.4	-5.981	-4.454	3.514.	-9.41	1.549
	$\mathbf{R^2}$	0.983**	0.901*	0.854*	0.990**	0.929**	0.945**	0.980**	0.913*	0.967*	0.946**

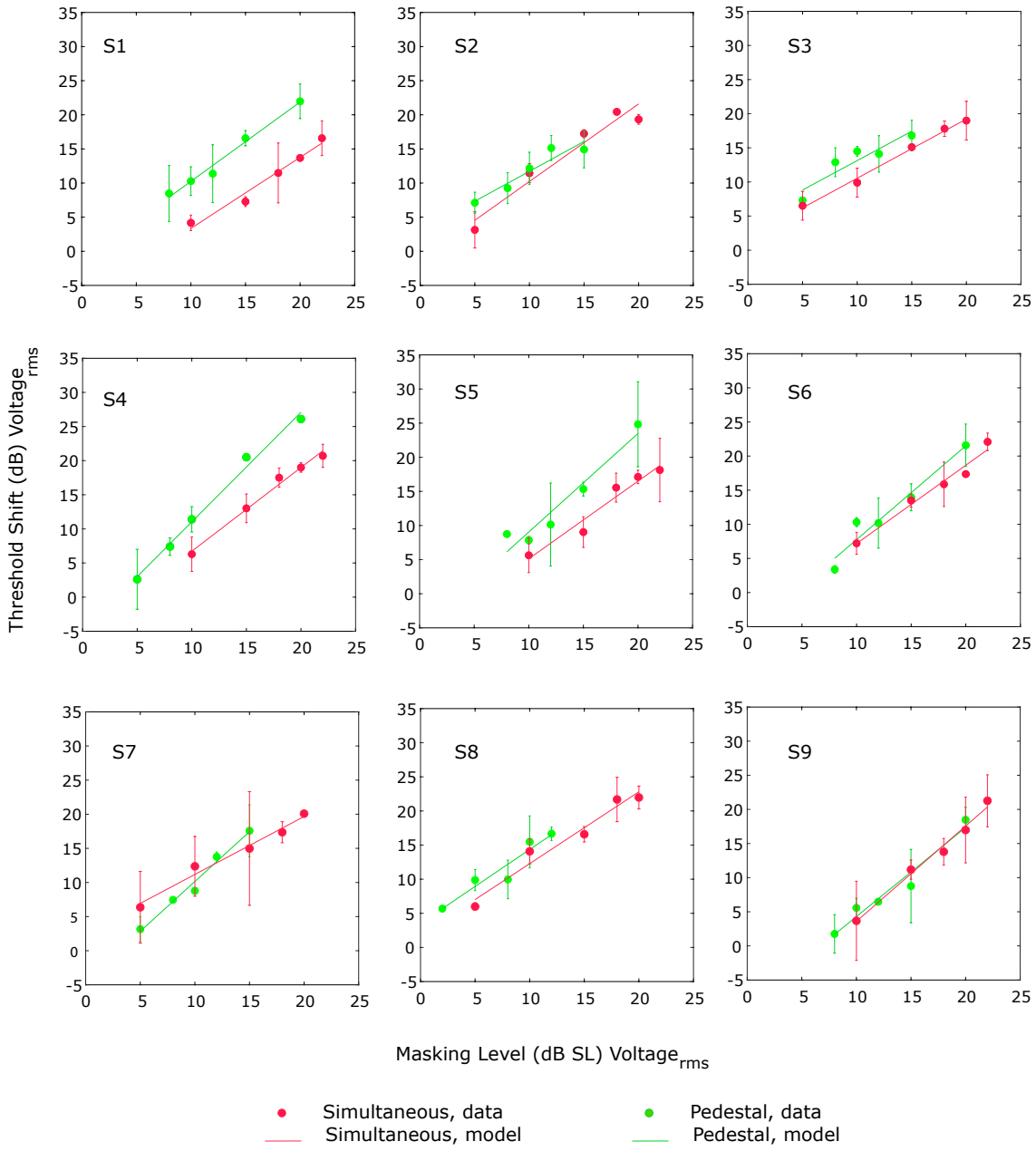

Figure 4.11: Results of the simultaneous and pedestal masking experiments for each subject. The resultant threshold shifts (dB) were plotted against the masking level (dB SL). Linear functions were fitted to the experimental data (see Table 4.4). The error bars indicate the standard deviations.

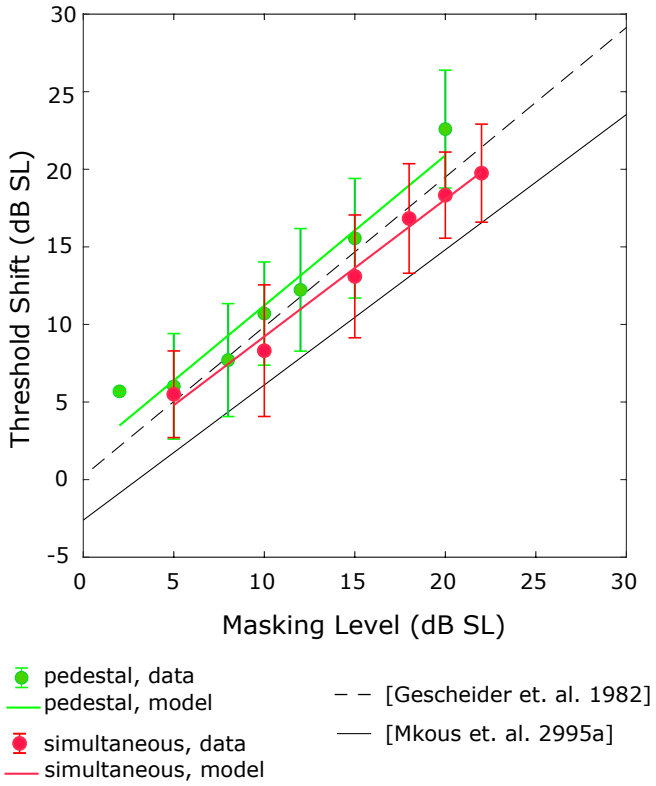

Figure 4.12: Threshold shifts obtained in pedestal and simultaneous masking experiments (data averaged across subjects). Linear curve-fit models are compared to those reported in the literature. The error bars indicate the standard deviations.

4.2.3 Results of Sharpness Experiments

In sharpness experiments, subjects compared different edge configurations prepared by integrating a 125 Hz sinusoidal signal with narrow band noise (test signal) to the simple edge which only contained a 125 Hz sinusoidal signal. The results given in Fig. 4.13 are based on percentage of trials in which either the simple edge (blue bar) or the test signal (pink bar) was detected sharper.

The test signals containing high-frequency background noise (E+PM1, E+PM2, E+PM3: in-channel pedestal masking) were felt significantly less sharper than the simple edge (E). Moreover, increasing high-frequency masking level decreased the perceived sharpness of the edges (p-values were <0.01, <0.001, and <0.001 for 5, 10 and 15 dB SL masking levels respectively). On the other hand, simultaneous

Table 4.5: Linear Mixed Model Results

Parameter	**Estimate**	**Standard Error**	**df**	**t**	**p-val**
Intercept	-3.75	1.17	17.804	-3.185	<0.01
Masking Type	2.82	0.467	62.724	6.050	<0.01
Masking Level	1.14	0.05	17.35	22.719	<0.01

masking (SM1-SM3) did not affect the perceived sharpness of the edges regardless of the masking level (p-values were 1, 0.449, 0.27 for 5, 10, 15 dB SL masking levels respectively). However, displaying the standard pedestal masking in decreasing ramp form (R) reduced the difference between simple edge with no masking and masked edge (p-value = 0.03). Although the RMS amplitude of both test signals in standard pedestal form (E+PM3) and ramp form (E+R) in-channel masking were equal, the percentage of trials in which ramp form was felt sharper than the simple edge was significantly higher than that of the standard one (compare pink bars of E+PM3 vs E+R, p-value<0.001). On the other hand, the test signal containing low-frequency background noise (E+PML: off-channel pedestal masking) was perceived as sharp as the simple edge (p-value = 0.32). This application shows that psychophysical masking in a particular channel can alter perception of a supra-threshold stimulus which can be used to render complex haptic sensations.

4.3 Discussion

4.3.1 Conventional Tactile Displays

Earlier studies with conventional tactile displays had also studied vibrotactile masking mostly regarding pattern recognition in humans. One of the first tactile displays used for this purpose was Optacon device. It was created as a reading aid for the blind and consisted of 6x24 vibrotactile pins. In [Craig, 1976], Craig investigated recognition of alphabet letters displayed by the Optacon. He asked subjects to recognize target

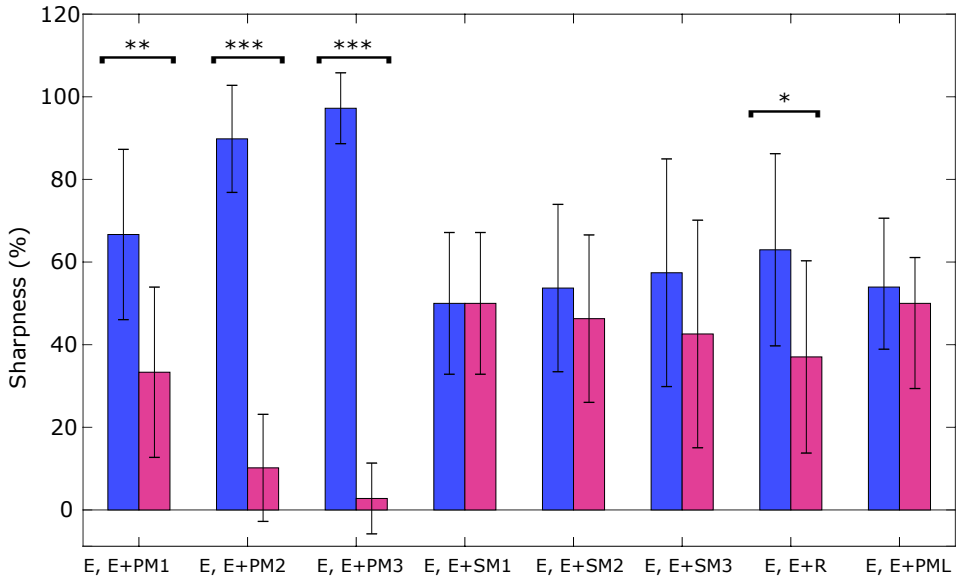

Figure 4.13: The percentage of trials in which either the simple edge (blue bar) or the test signal (pink bar) was detected sharper. The error bars indicate the standard deviations. Significantly different comparisons are marked by asterisks (* p-val<0.05, ** p-val <0.01, *** p-val<0.001).

letters in presence of a masking stimulus (another letter) presented before or after the test stimulus. He found that backward masking interfered with letter recognition more than forward one. In addition, the recognition accuracy improved as the time interval between target letter and the masking stimuli (ISI) was increased. In line with this study, Craig and Evans [Craig and Evans, 1987] studied the persistence of tactual features in memory. They displayed tactile lines using Optacon and asked subjects to count the number of lines in the target patterns displayed with masking patterns with varying time gaps. The subjects often overestimated the number of lines in the target patterns. These results showed that vibrotactile patterns can persist in memory for relatively long durations (see however [Güçlü and Murat, 2007]).

Researchers also studied vibrotactile masking to investigate information transfer capabilities of vibrotactile actuators. Tan et. al. [Tan et al., 2003] examined temporal masking of stimuli with sinusoidal mixtures using Tactuator device. The device consisted of three independent, point-contact, one-degree-of-freedom actuators interfaced

individually with the fingerpads of the thumb, index finger, and middle finger. The authors composed seven different stimuli by adding low (2, 4 Hz), medium (30 Hz), and high (300 Hz) frequencies for two signal durations (125 or 250 ms). They asked subjects to identify target signals displayed under three masking conditions (forward, backward and sandwich). The pattern identification success of the subjects was good and similar in forward and backward masking but poor in sandwich masking. Additionally, their results showed that optimal delivery rate of target signals decreased as stimulus duration and size of the stimulus set were increased.

Enriquez and McLean investigated the backward and common-onset masking characteristics of simple vibrotactile stimuli using a custom designed display. They integrated two Tactaid tactile displays (voice-coil based transducers) to deliver tactile stimuli to middle and ring fingers of these subjects simultaneously or consecutively. They tested the identification of 250 Hz sinusoidal waveforms displayed at 250 Hz, at fixed amplitude in varying durations and ISI. They found that common-onset masking exhibited a significantly larger masking effect than backward.

Recently, investigators also studied masking to deliberately attenuate the tactile sensations in different applications. For example, Asano et. al. [Asano et al., 2015] modified the perceived roughness of textured surfaces by displaying a simultaneous vibrotactile stimuli via a voice coil actuator worn on the finger. Kim et. al. [Kim et al., 2012] studied masking of key-click feedback signals on a flat surface for ten-finger touch. They hypothesised that even if the flat surface was vibrated entirely, the subjects could feel localized key-click feedback on their active fingers with a sufficient masking effect on the others. They found that, masking effect was stronger when two fingers of the same hand interacted with the surface compared to the case of index fingers of both hands were involved.

Our results showed that electrovibration is similar to conventional tactile displays in terms of masking effects. However, the displays listed above have some technical limitations which confine their usage in future applications. For example, the haptic feedback is limited by the number of pins or actuator speed and bandwidth. Therefore,

it is hard to present complex and multiple stimuli using these devices. As they also lack visual information, they cannot be integrated easily with other devices such as computer screens, phones or tablets. On the other hand, in electrovibration, the haptic stimuli is displayed on a flat surface without any moving parts. It is quite easy to generate complex tactile stimuli using electrovibration on large scale surfaces and even small portable devices. Additionally, it is also a promising technology in terms of designing multi-finger applications. However, the users need to move their fingers to feel the haptic feedback generated by electrovibration.

4.3.2 Previous Vibrotactile Masking Studies

We found that the electrovibration detection thresholds of sinusoidal stimulus were elevated as a linear function of masking level for both masking types. The slopes for subject average data were 0.88 and 0.97 for simultaneous and pedestal masking respectively. Nonetheless, the individual slopes were varied between 0.867 to 1.397 for simultaneous masking and 0.861 to 1.606 for pedestal one. It is interesting to note that similar results were also obtained in earlier vibrotactile studies (see Fig. 4.12). Gescheider et. al. [Gescheider et al., 1982] reported masking functions with a slope of approximately 1.0 when narrow-band, high frequency noise was used to mask the detection of a high frequency sinusoidal test stimulus in pedestal masking. Makous [Makous et al., 1995a] conducted simultaneous masking experiments and measured the threshold shifts for a high frequency sinusoidal test stimulus applied with high-frequency narrow band noise masking stimulus. The thresholds were elevated as a linear function of masking level with an approximate slope of 1.1. In the vibrotactile studies above both masking and test stimuli were indeed delivered to stationary fingers in the normal direction. On the contrary, in our case, the mechanical effects of both masking and test stimuli were delivered to moving fingers in the tangential direction. The similarity in the slopes of masking functions obtained by electrovibration and normal vibrotactile stimulation suggest that similar psychophysical channels were recruited for detection. However, in [Yıldız et al., 2015], Yıldız et al. showed that

movement produce a gating effect in detection, especially at high speeds. Although both passive and active movement elevated thresholds in the fast speed range, the effect of forward masking was constant as the movement condition varied. The speeds used in the electrovibration study reported here were lower than the fast speed range in the gating study. Therefore there was probably not much gating effect and the masking functions were similar to those reported previously.

Our results showed that pedestal masking is more effective (i.e. larger shift in threshold, and higher slope) than simultaneous masking in electrovibration. It is well known that masking and test stimuli durations are important for the masking effect as mentioned in Section 2.1.2. When we investigate threshold shifts for pedestal and simultaneous masking as a function of masking duration, the results are comparable with previous vibrotactile literature [Gescheider et al., 1995]. Gescheider et. al. reported that the tactile thresholds for detecting a 50 ms signal, presented 25 ms after the termination of a masking stimulus, increased as a function of masking amplitude and duration. This situation involves temporal summation. Temporal summation is a phenomenon which occurs due to integration of neural responses which reduce thresholds [Gescheider et al., 1999], [Gescheider et al., 1995], [Gescheider et al., 1994]. Just like spatial summation, i.e. decrease of thresholds due to increased contact area [Yıldız and Güçlü, 2013], temporal summation is an exclusive property of the psychophysical P channel. We would expect a similar phenomenon due to masking duration in electrovibration as well. In other words, if the masking duration was increased (in the pedestal condition), we would expect a higher masking effect. If one assumes the simultaneous masking as a shortened pedestal masking stimulus, we observe a similar trend.

4.3.3 Perception of Edge Sharpness and Textures

We observed that, displaying edges with in-channel pedestal masking stimuli decreased their perceived sharpness significantly as a function of masking level. Nonetheless, simultaneous masking did not affect the sharpness perception. It is important

to note that the edge stimulus was a supra-threshold sinusoidal wave, therefore the masking functions presented in the results (Fig. 4.11 and Fig. 4.12) do not readily apply here. Therefore sharpness perception, which requires supra-threshold stimuli may be more easily explained based on the contrast between background and foreground stimuli. Increasing the level of pedestal masking in our experiments decreased the contrast between the edge and the background. Since the background stimuli were always zero for edges displayed with simultaneous masking, they were perceived equally despite the differences in masking amplitudes. Our results suggest that frequency depended psychophysical channels also play a role in the resultant contrast. In fact, despite its high level background stimuli, the sharpness of the edge displayed with a low frequency pedestal masking (E+PML) was perceived similar to that of simple edge with no masking. This is because the low frequency pedestal masking stimulus is off-channel, in other words does not activate the Pacinian channel appreciably.

The gray scale images given in Fig. 4.5 show this paradigm better. Since the intensity of these images was adjusted based on amplitude of electrostatic forces for simplicity, the sharpness of the images perceived visually do not exactly match with the perceived haptic sharpness measured in our experiments. In a real application, the intensities should also be normalized by considering the frequency-dependent sensitivity of human haptic perception. In general our results suggest that sharpness perception depends on local effects, and sharper edges can be rendered by reshaping the continuous background stimuli into a ramped one (compare E and E+R in Fig. 4.13, and Fig. 4.5). Similar relationship between contrast and perceived edge sharpness has been also observed in visual studies [Schreiber, 1993]. Increasing the local visual contrast between an edge and its surroundings enhances the perceived sharpness. This local visual contrast value is a function of both spatial frequency and luminance, regarding the edge and its surroundings [Peli, 1990, Simone et al., 2012].

4.3.4 Predicting Electrovibration Thresholds

The subjects showed similar sensitivity to sinusoidal and narrow band noise voltage signal used in our study. This was because the stimuli were adjusted to get the same peak energies in the spectral components after the model in Chapter 3. The detection of electrovibration stimuli depends on electrical properties of human skin, electrostatic force generation due to capacitance coupling, and human psychophysical sensitivity. To estimate the spectral energies which activate psychophysical channels, we first computed the electrostatic forces for the applied voltage signal using the circuit model in Chapter 3. The force output from the model is analyzed in the frequency domain. The force signal due to sinusoidal excitation contains only one frequency component at 250 Hz, whereas the one due to narrow band noise excitation contains many components (see Fig. 4.3). However, as the electrostatic force formula is nonlinear, it is difficult to predict the components in complex stimuli without running the model. Furthermore, the spectral components need to be weighted according to human psychophysical sensitivity. Our results show that the thresholds produced spectral components in the range of 200-300 Hz (see Fig. 4.10). Therefore the Pacinian psychophysical channel was most likely recruited for detection.

It is important to note that we used the average human sensitivity curve reported in Chapter 3, however there will be a variation between subjects from a psychophysical point of view as well as due to other experimental factors such as the movement direction, angle of contact, skin temperature, skin moisture as pointed out in [Adams et al., 2013, Delhaye et al., 2014, Pasumarty et al., 2011, Derler and Gerhardt, 2012, Andre et al., 2011, Derler et al., 2009]. For example, in our study, within-subject variation of thresholds changed between 1 dB (S6) to 12 dB (S2). Moreover, there was a 7 dB between-subject variation in terms of average threshold results. This subject-to-subject variability might be caused by the differences in finger size, electromechanical properties, moisture, and neural adaptation.

Chapter 5

CONCLUSIONS AND FUTURE DIRECTIONS

5.1 Conclusions

Electrovibration is one of the emerging technologies to generate realistic haptic feedback on touch screens. Although the technology for rendering haptic effects on touch surfaces using electrovibration is already in place, our knowledge of the perception mechanisms behind these effects is limited. In this thesis, we investigated haptic perception of electrovibration displayed on touch screens in two different aspects: effects of input signal properties and masking.

In Chapter 3, we investigated how input voltage waveform affects our haptic perception of electrovibration on touch screens. Through psychophysical experiments with eight subjects, we first measured the detection thresholds of electrovibration stimuli generated by sinusoidal and square voltages at various frequencies. We observed that the subjects were more sensitive to square wave stimuli than sinusoidal one for fundamental frequencies lower than 60 Hz. We hypothesized that the sensation difference of waveforms in low fundamental frequencies is due to frequency-dependent electrical properties of human skin and human tactile sensitivity. To validate our hypothesis and observe if there was any other physical factor which may affect our perception of electrovibration perception, we conducted a second experiment with another group of eight subjects. We collected force and acceleration data from fingertips of the subjects while they explored a touch screen displaying electrovibration stimuli at threshold voltages. We analyzed the collected data in frequency domain by taking the human tactile sensitivity curves given in [Morioka and Griffin, 2005, Hatzfeld et al., 2016] into account. The results suggested that Pacinian was the primary psychophysical channel in the detection of the square wave input signals tested in this

study. Moreover, our results showed that measured acceleration and force data are affected by finger scan speed.

To the best of our knowledge, this is the first detailed study investigating the effect of input voltage waveform on haptic perception of electrovibration. Our findings not only help us to understand the mechanism of human tactile sensing of electrovibration but also may help engineers and designers to develop applications displaying tactile effects to the users through a touch screen. For example, a user interface developer designing a virtual dial on a touch screen may prefer to use low frequency square pulses rather than sinusoidal ones to display tactile dents. On the other hand, less detectable sinusoidal signals could be used to display frictional feedback to the user while she/he turns the dial on the screen for better control. Furthermore, the perception difference between waveforms may also be used for pattern and edge recognition. When a visually impaired user explores a virtual shape on a touch screen, the edges can be conveyed by low-frequency square waves while a sinusoidal wave can be used for smoother feeling inside. Moreover, since the detection of tactile stimuli is determined by frequency components below 1kHz, it may not be necessary to transmit higher frequency components which would be lower than the detection thresholds. This ensures transmission of less data without sacrificing the perceptual needs for systems with limited bandwidth.

Furthermore, the results of this study can be a guide for developing an electromechanical model of human finger linking the electrostatic force displayed to human finger pad by electrovibration to the mechanical forces felt at the finger contact interface. As our results suggest, frictional forces modulated by the contact interface and scan speed have influence on mechanical vibrations measured at fingertip and hence potentially on our tactile perception. Finally, our results also suggest that tactile perception of electrovibration is similar to that of vibrotactile stimuli.

In Chapter 4, we investigated the effect of masking on tactile perception of electrovibration displayed on touch screens. We measured the masked thresholds of sinusoidal bursts (125 Hz) using simultaneous and pedestal masking. The masking stimuli

were narrow-band noise bursts (covering a frequency range of 75-200 Hz), applied at five different levels varying from 2 to 22 dB SL. For each subject, the detection thresholds were elevated as a linear function of mask level under both masking conditions as observed in earlier vibrotactile studies, which is a very different modality with stationary finger and normal forces. We also observed that the pedestal masking was more effective (i.e higher threshold shift and slope) than simultaneous masking. To investigate the effect of tactile masking on our haptic perception of edge sharpness, we compared the perceived sharpness of the edges separating two textured regions displayed with and without various masking stimuli. Our results suggest that sharpness perception depends on the local contrast between background and foreground stimuli, which is a function of both masking amplitude and activation levels of frequency dependent psychophysical channels.

To the best of our knowledge, this is the first detailed masking study conducted on touch screens where the stimuli were delivered to moving fingers on the tangential direction. The consistency between our results and former vibrotactile studies can open doors to new applications of masking. We can, for example, investigate masking on multiple fingers, masking on fingers on different hands, and masking with electrovibration and some other vibrotactile stimulus. Moreover, haptic display designers can benefit from our findings to develop applications involving geometrical shapes with texture. Through our masking functions, they can, for example, estimate the maximum amplitude of the background texture to display a shape that is still detectable by human finger. They can also augment the sharpness of its edges by creating a local contrast. For example, our study shows that one can decrease the amplitude of electrovibration gradually near the edges at the background to make edges feel sharper. Alternatively, one can augment the sharpness of edge by using a high-frequency electrovibration signal as the edge and low-frequency signal as the background, instead of a high frequency background.

5.2 Future Directions

In this section, the possible future directions related to this thesis topic are listed.

5.2.1 Modelling

In our study, we have interpreted the simulation and experimental results based on the generated electrostatic force in the normal direction. However, when there is no relative movement between the surface and the finger, the electrostatic force, albeit varying in time with sinusoidal excitation, does not generate a tactile sensation. It is accepted that the electrostatic force changes the normal force, and thus friction during movement. The mechanoreceptors in the skin are probably excited by shear forces modulated by friction. Therefore, a physically accurate explanation of electrovibration can only be obtained by an electromechanical model linking the electrostatic force generation at the tissues and the mechanical forces of movement. As a future work, the electrical model can be extended by combining it with the mechanical properties of the finger.

5.2.2 Masking

In this thesis, both masking and test stimuli were selected to activate the Pacinian channel. The masking effect can also be investigated by using mask and test stimuli selected to activate other channels. Moreover, investigation of other masking types such as forward and backward masking can be another interesting research path.

5.2.3 Perception of Complex Stimuli

In this thesis, we only investigated the effect of input signal properties and masking on the haptic perception of electrovibration. However, the perception of other complex electrovibration stimuli such as textures and shapes still needs comprehensive research.

5.2.4 Haptic Contrast

Although our results suggest that sharpness perception depends on the local contrast between background and foreground stimuli, quantification of this contrast is not pursued in this study. Currently, we are working on defining a value for local haptic contrast.

5.2.5 Multi-Finger Systems

In this thesis, we used a single-touch display in which the generated electrostatic force is equal on the whole surface. Therefore, it is not possible to actuate multi-fingers by different stimuli using the current touchscreen. For the applications which may require gesture-based multi-touch interactions, the current touch screen should be produced by combining multi-electrodes.

5.2.6 Multi-Modal Systems

In this thesis, we considered only electrovibration as an actuation method. However, hybrid systems combining mechanical and electrostatic actuation can enhance the variety of generated haptic effects. For example, mechanical actuation of the touch screen can create a button click effect which cannot be created on an electrostatic display without a finger motion.

5.2.7 Optimization of Touch Screen

In our research, we used 3M MicroTouch display as a touchscreen. This display is produced for sensation purposes only without consideration of haptic applications. As a future work, a new touchscreen can be designed to maximize the force output with less voltage/current input by optimizing the insulator, conductor, and surface roughness parameters. Moreover, design of a new touch screen which is capable of sensing and actuation simultaneously is another research problem.

BIBLIOGRAPHY

[Adams et al., 2013] Adams, M. J., Johnson, S. A., Lefèvre, P., Lévesque, V., Hayward, V., André, T., and Thonnard, J.-L. (2013). Finger pad friction and its role in grip and touch. *Journal of The Royal Society Interface*, 10(80), DOI: 10.1098/rsif.2012.0467.

[Agarwal et al., 2002] Agarwal, A. K., Namni, K., Kaczmarek, K. A., Tyler, M. E., and Beebe, D. J. (2002). A hybrid natural/artificial electrostatic actuator for tactile stimulation. In *Proc. of the 2nd Annual Conference on Microtechnologies in Medicine and Biology*, pages 341–345, Madison, Wisonsin USA.

[Aiello, 1998] Aiello, G. (1998). Multidimensional electrocutaneous stimulation. *IEEE Transactions on Rehabilitation Engineering*, 6(1):95–101.

[Andre et al., 2011] Andre, T., Levesque, V., Hayward, V., Lefevre, P., and Thonnard, J. (2011). Effect of skin hydration on the dynamics of fingertip gripping contact. *Journal of Royal Society Interface*, 8:1574–1583, DOI:10.1098/rsif.2011.0086.

[Asano et al., 2015] Asano, S., Okamoto, S., and Yamada, Y. (2015). Vibrotactile stimulation to increase and decrease texture roughness. *IEEE Transactions on Human-Machine Systems*, 45(3):393–398.

[Bau et al., 2010] Bau, O., Poupyrev, I., Israr, A., and Harrison, C. (2010). Teslatouch: Electrovibration for touch surfaces. In *Proc. of the 23nd annual ACM symposium on User interface software and technology (UIST'10)*, pages 283–292, NewYork, USA.

[Beebe et al., 1995] Beebe, D., Heymel, C., Kaczmarek, K., and Tyler, M. (1995). A polyimide-on-silicon electrostatic fingertip tactile display. In *Proc. of the IEEE 17th Annual Conference on Engineering in Medicine and Biology Society*, pages 1545–1546.

[Bensmaia and Hollins, 2011] Bensmaia, S. and Hollins, M. (2011). The vibrations of texture. *Somatosensory and Motor Research*, 20(1):33–43.

[Biet et al., 2008] Biet, M., Casiez, G., Girau, F., and Lemaire-Semail, B. (2008). Discrimination of virtual square gratings by dynamic touch on friction based tactile displays. In *Symposium on Haptics Interfaces for Virtual Environment and Teleoperator Systems*, pages 41–48.

[Bolanowski et al., 1988] Bolanowski, S., Gescheider, G., Verrillo, R. T., and Checkosky, C. (1988). Four channels mediate the mechanical aspects of touch. *Acoustic Society of America*, 84(5):1680–1694.

[Cholewiak et al., 2010] Cholewiak, S. A., Kim, K., Tan, H. Z., and Adelstein, B. D. (2010). A frequency domain analysis of haptic gratings. *IEEE Transactions on Haptics*, 3(1):3–14.

[Craig, 1976] Craig, J. (1976). Vibrotactile letter recognition: The effects of a masking stimulus. *Perception & Psychophysics*, 20(5):317–326.

[Craig and Evans, 1987] Craig, J. and Evans, P. (1987). Vibrotactile masking and the persistence of tactual features. *Perception & Psychophysics*, 42(4):309–317.

[Delhaye et al., 2014] Delhaye, B., Lefèvre, P., and Thonnard, J.-L. (2014). Dynamics of fingertip contact during the onset of tangential slip. *Journal of The Royal Society Interface*, 11(100), `DOI:10.1098/rsif.2014.0698`.

[Demarest, 1998] Demarest, K. R. (1998). *Engineering Electromagnetics*. Prentice Hall.

[Derler and Gerhardt, 2012] Derler, S. and Gerhardt, L. (2012). Tribology of skin: review and analysis of experimental results for the friction coefficient of human skin. *Tribology Letters*, 45:1–27.

[Derler et al., 2009] Derler, S., Gerhardt, L.-C., Lenz, A., Bertaux, E., and Hadad, M. (2009). Friction of human skin against smooth and rough glass as a function of the contact pressure. *Tribology International*, 42:1565–1574.

[Ehrenstein and Ehrenstein, 1999] Ehrenstein, W. H. and Ehrenstein, A. (1999). Psychophysical methods. In *Modern Techniques in Neuroscience Research*, pages 1211–1241. Springer Berlin Heidelberg.

[Enriquez and MacLean, 2008] Enriquez, M. and MacLean, K. (2008). Backward and common-onset masking of vibrotactile stimuli. *Brain Research Bulletin*, 75:761–769.

[Fagiani and Barbieri, 2014a] Fagiani, R. and Barbieri, M. (2014a). Modeling of finger-surface contact dynamics. *Tribology International*, (74).

[Fagiani and Barbieri, 2014b] Fagiani, R. and Barbieri, M. (2014b). Modelling of finger-surface contact dynamics. *Tribology International*, 74:130–137.

[Fagiani et al., 2011] Fagiani, R., Massi, F., Chalet, E., Berthier, Y., and Akay, A. (2011). Tactile perception by friction induced vibrations. *Tribology International*, 44:1100–1110.

[Gescheider et al., 1999] Gescheider, G., Berryhill, M., Verrillo, R., and Bolanowski, S. (1999). Vibrotactile temporal summation: probability summation or neural integration? *Somatosensory & Motor Research*, 16:229–242.

[Gescheider et al., 2001] Gescheider, G., Bolanowski, S., and Hardick, K. (2001). The frequency selectivity of information-processing channels in the tactile sensory systems. *Somatosensory and Motor Research*, 18:191–201.

[Gescheider et al., 1989] Gescheider, G., Bolanowski, S., and Verrillo, R. (1989). Vibrotactile masking: Effects of stimulus onset asynchrony and stimulus frequency. *The Journal of Acoustical Society of America*, 85:2059–2064.

[Gescheider et al., 1994] Gescheider, G., Hoffman, E., Harrison, M., Travis, M., and Bolanowski, S. (1994). The effects of masking on vibrotactile temporal summation in the detection of sinusoidal and noise signals. *The Journal of Acoustical Society of America*, 95:1006–1016.

[Gescheider et al., 1983] Gescheider, G., Malley, J., and Verrillo, R. (1983). Vibrotactile forward masking: Evidence for channel independence. *The Journal of Acoustical Society of America*, 74:474–485.

[Gescheider and Migel, 1995] Gescheider, G. and Migel, N. (1995). Vibrotactile forward masking 2: Some temporal parameters in vibrotactile forward masking. *The Journal of Acoustical Society of America*, 98:3195–3199.

[Gescheider et al., 1995] Gescheider, G., Santoro, E., Makous, J., and Bolanowski, S. (1995). Vibrotactile forward masking 1: Effects of the amplitude and duration of the masking stimulus. *The Journal of Acoustical Society of America*, 98:3188–3194.

[Gescheider et al., 1982] Gescheider, G., Verrillo, R., and Doren, C. V. (1982). Prediction of vibrotactile masking functions. *The Journal of Acoustical Society of America*, 72:1421–1426.

[Gescheider et al., 2002] Gescheider, G. A., Bolanowski, S. J., Pope, J. V., and Verrillo, R. T. (2002). A four-channel analysis of the tactile sensitivity of the fingertip: frequency selectivity, spatial summation, and temporal summation. *Somatosensory and Motor Research*, 19(2):114–124.

[Gescheider et al., 2009] Gescheider, G. A., Wright, J., and Verrillo, R. (2009). *Information-processing channels in the tactile sensory system a psychophysical and psysiological analysis*. Psychology Press.

[Gilson, 1969] Gilson, R. D. (1969). Vibrotactile masking: Some spatial and temporal aspects. *Perception & Psychophysics*, 5(3):176–180.

[Grimnes, 1983a] Grimnes, S. (1983a). Electrovibration, cutaneous sensation of microampere current. *Acta Physiol Scand*, 118:1565–1574.

[Grimnes, 1983b] Grimnes, S. (1983b). Skin impedance and electro-osmosis in the human epidermis. *Medical & Biological Engineering & Computing*, 21:739–749.

[Güçlü, 2007] Güçlü, B. (2007). Deviation from Weber's law in the non-pacinian i tactile channel: A psychophysical and simulation study of intensity discrimination. *Neural Computation*, 19(10):2638–2664.

[Güçlü and Bolanowski, 2003] Güçlü, B. and Bolanowski, S. (2003). Frequency responses of cat rapidly adapting mechanoreceptive fibers. *Somatosensory & Motor Research*, 20:249–263.

[Güçlü and Bolanowski, 2004] Güçlü, B. and Bolanowski, S. (2004). Probability of stimulus detection in a model population of rapidly adapting fibers. *Neural Computation*, 16(1):39–58.

[Güçlü and Bolanowski, 2005a] Güçlü, B. and Bolanowski, S. (2005a). Vibrotactile thresholds of the non-pacinian I channel: I. methodological issues. *Somatosensory & Motor Research*, 22:49–56.

[Güçlü and Bolanowski, 2005b] Güçlü, B. and Bolanowski, S. (2005b). Vibrotactile thresholds of the non-pacinian I channel: II. predicting the effects of contactor location on the phalanx. *Somatosensory and Motor Research*, 22(1/2):57–68.

[Güçlü et al., 2005] Güçlü, B., Bolanowski, S., and Istefanopulos, Y. (2005). Population-response model for vibrotactile spatial summation. *Somatosensory Motor Research*, 22(4):239–253.

[Güçlü et al., 2014] Güçlü, B., Çelik, S., and Ilci, C. (2014). Representation of haptic objects during mental rotation in congenital blindness. *Perceptual & Motor Skills*, 118:587–607.

[Güçlü and Ş.M. Dinçer, 2013] Güçlü, B. and Ş.M. Dinçer (2013). Neural coding in the non-pacinian I tactile channel: A psychophysical and simulation study of magnitude estimation. *Somatosensory Motor Research*, 30(1):1–15.

[Güçlü and Murat, 2007] Güçlü, B. and Murat, A. (2007). Active touch does not improve sequential processing in a counting task. *Acta Neurobiologiae Experimentalis*, 67:167–169.

[Güçlü and Öztek, 2007] Güçlü, B. and Öztek, C. (2007). Tactile sensitivity of children: Effects of frequency, masking, and the non-pacinian I psychophysical channel. *Journal of Experimental Child Psychology*, 98:113–130.

[Hamer et al., 1983] Hamer, R. D., Verrillo, R., and Zwislocki, J. (1983). Vibrotactile masking of pacinian and non-pacinian channels. *The Journal of Acoustical Society of America*, 73:1293–1303.

[Hatzfeld et al., 2016] Hatzfeld, C., Cao, S., Kupnik, M., and Werthschtzky, R. (2016). Vibrotactile force perception - absolute and differential thresholds and external influences. *IEEE Transactions on Haptics*, 9(4):586–597.

[Ide and Hidaka, 2013] Ide, M. and Hidaka, S. (2013). Tactile stimulation can suppress visual perception. *Scientific Reports*, `DOI:10.1038/srep03453`.

[Ilkhani et al., 2017] Ilkhani, G., Aziziaghdam, M., and Samur, E. (2017). Data-driven texture rendering on an electrostatic tactile display. *International Journal of HumanComputer Interaction*, 33(9):756–770, DOI:10.1080/10447318.2017.1286766.

[Johnsen and Rahbek, 1923] Johnsen, A. and Rahbek, K. (1923). A physical phenomenon and its applications to telegraphy, telephony, etc. *IEE Journal*, 61:713–725.

[Jones and Sarter, 2008] Jones, L. and Sarter, N. (2008). Tactile displays: guidance for their design and application. *Human Factors: The Journal of the Human Factors and Ergonomics Society*, 50(90):90–111.

[Kaczmarek et al., 2006] Kaczmarek, K., Nammi, K., Agarwal, A., Tyler, M., Haase, S., and Beebe, D. (2006). Polarity effect in electrovibration for tactile display. *IEEE Transactions on Biomedical Engineering*, 53(10):2047–2054.

[Kaczmarek et al., 1991] Kaczmarek, K., Webster, J., Rita, P., and Tompkins, W. (1991). Electrotactile and vibrotactile displays for sensory substitution systems. *IEEE Transactions on Biomedical Engineering*, 38(1).

[Kang et al., 2017] Kang, J., Kim, H., Choi, S., Kim, K. D., and Ryu, J. (2017). Investigation on low voltage operation of electrovibration display. *IEEE Transactions on Haptics*, 10(3):371–381.

[Kim et al., 2015] Kim, H., Kang, J., Kim, K., Lim, K., and Ryu, J. (2015). Method for providing electrovibration with uniformed density. *IEEE Transactions on Haptics*, 8(4):492–496.

[Kim et al., 2012] Kim, J., Dai, X., Cao, X., Picciotto, C., Tan, D., and Tan, H. (2012). A masking study of key-click feedback signals on a virtual keyboard. In *Eurohaptics 2012, Part I, LNCS 7282*, pages 247–257.

[Kim et al., 2013] Kim, S., Israr, A., and Poupyrev, I. (2013). Tactile rendering of 3d features on touch surfaces. pages 531–538, St. Andrews. UIST'13.

[Kuroki et al., 2017] Kuroki, S., Watanabe, J., and Nishida, S. (2017). Integration of vibrotactile frequency information beyond the mechanoreceptor channel and somatotopy. *Scientific Reports*, DOI:10.1038/s41598-017-02922-7.

[Landau and Everitt, 2004] Landau, S. and Everitt, B. (2004). *A Handbook of Statistical Analyses using SPSS*. Chapman & Hall/CRC.

[Leek, 2001] Leek, M. R. (2001). Adaptive procedures in psychophysical research. *Perception and Psychophysics*, 63(8):1279–1292.

[Levitt, 1971] Levitt, H. (1971). Transformed up-down methods psychoacoustics. *The Journal of Acoustical Society of America*, 49(2):467–477.

[Makous et al., 1995a] Makous, J., Friedman, R., and C.J. Vierck, J. (1995a). A critical band filter in touch. *The Journal of Neuroscience*, 15(4):2808–2818.

[Makous et al., 1995b] Makous, J., Gescheider, G., and Bolanowski, S. (1995b). Decay in the effect of vibrotactile masking. *The Journal of Acoustical Society of America*, 99(2):1124–1129.

[Mallinckrodt et al., 1953] Mallinckrodt, E., Hughes, A., and Sleator, W. (1953). Perception by the skin of electrically induced vibrations. *Science*, 118:277–278.

[Mayer et al., 2013] Mayer, D., Peshkin, M., and Colgate, E. (2013). Fingertip electrostatic modulation due to electrostatic attraction. In *Proc. IEEE World Haptics Conference (WHC'13)*, pages 43–48, Daejeon, South Korea.

[Morioka and Griffin, 2005] Morioka, M. and Griffin, M. (2005). Thresholds for the perception of hand-transmitted vibration: Dependence on contact area and contact location. *Somatosensory and Motor Research*, 22(4):281–297.

[Mullenbach et al., 2017] Mullenbach, J., Peshkin, M., and Colgate, E. (2017). eshiver: Lateral force feedback on fingertips through oscillatory motion of an electroadhesive surface. *IEEE Transactions on Haptics*, 10(3):358–370.

[Nakamura and Yamamoto, 2016] Nakamura, T. and Yamamoto, A. (2016). A multi-user surface visuo-haptic display using electrostatic friction modulation and capacitive-type position sensing. *IEEE Transaction on Haptics*, 9(3):311–322.

[Nakamura and Yamamoto, 2017] Nakamura, T. and Yamamoto, A. (2017). Modeling and control of electroadhesion force in dc voltage. *ROBOMECH Journal*, 4(1):18, ISSN: 2197-4225, DOI:10.1186/s40648-017-0085-3.

[Osgouei et al., 2017] Osgouei, R., Kim, J., and Choi, S. (2017). Improving 3d shape recognition with electrostatic friction display. *IEEE Transactions on Haptics*, DOI: 10.1109/TOH.2017.2710314.

[Pasumarty et al., 2011] Pasumarty, S. M., Johnson, S. A., Watson, S. A., and Adams, M. J. (2011). Friction of the human finger pad: influence of moisture, occlusion and velocity. *Tribology Letters*, 44:117–127.

[Peli, 1990] Peli, E. (1990). Contrast in complex images. *Journal of Optical Society of America*, 7(10):2032–2040.

[Saga and Raskar, 2013] Saga, S. and Raskar, R. (2013). Simultaneous geometry and texture display based on lateral force for touchscreen. In *IEEE World Haptics*, pages 437–442.

[Schreiber, 1993] Schreiber, W. (1993). *Fundamentals of Electronic Imaging Systems: Some Aspects of Image Processing*. Springer-Verlag.

[Shultz et al., 2013] Shultz, C. D., Peshkin, M., and Colgate, E. (2013). Surface haptics via electroadhesion: Expanding electrovibration by johnsen and rahbek. In *Proc. IEEE World Haptics Conference (WHC'15)*, pages 57–62.

[Simone et al., 2012] Simone, G., Pedersen, M., and Hardeberg, J. Y. (2012). Measuring perceptual contrast in digital images. *J. Vis. Commun. Image R.*, 23:491–506.

[Skedung, 2012] Skedung, L. (2012). *Tactile perception: Role of friction and texture*. PhD thesis, KTH Royal Institute of Technology.

[Strong and Troxel, 1970] Strong, R. and Troxel, D. (1970). An electrotactile display. *IEEE Transactions on Man-Machine Systems*, 11(1):72–79.

[Summers et al., 1997] Summers, I. R., Cooper, P. G., Wright, P., Gratton, D. A., Milnes, P. M., and Brown, B. H. (1997). Information from time-varying vibrotactile stimuli. *Journal of Acoustical Society of America*, 102(6):3686–3696.

[Tan et al., 2003] Tan, H., Reed, C., and Delhorne, L. (2003). Temporal masking of multidimensional tactual stimuli. *The Journal of Acoustical Society of America*, 114:3295–3308.

[Tang and Beebe, 1998] Tang, H. and Beebe, D. (1998). A microfabricated electrostatic haptic display for persons with visual impairments. *IEEE Transactions on Rehabilitation Engineering*, 6(3):241–248.

[Tang et al., 2015] Tang, W., Chen, N., and et al., J. Z. (2015). Characterization of tactile perception and optimal exploration movement. *Tribology Letters*, 58(28), DOI:10.1007/s11249-015-0507-4.

[Tashiro et al., 2009] Tashiro, K., Shiokawa, Y., Aono, T., and Maeno, T. (2009). Realization of button click feeling by use of ultrasonic vibration and force feedback. In *IEEE World Haptics Conference - Third Joint EuroHaptics conference and Symposium on Haptic Interfaces for Virtual Environment and Teleoperator Systems*, pages 1–6.

[Vardar et al., 2017a] Vardar, Y., Güçlü, B., and Basdogan, C. (2017a). Effect of waveform on tactile perception by electrovibration displayed on touch screens. *IEEE Transactions on Haptics*, 10(4):488–499.

[Vardar et al., 2017b] Vardar, Y., Güçlü, B., and Basdogan, C. (2017b). Tactile masking by electrovibration. *Submitted*.

[Vardar et al., 2017c] Vardar, Y., İşleyen, A., Saleem, M., and Basdogan, C. (2017c). Roughness perception of virtual textures displayed by electrovibration on touch screens. In *Proc. of IEEE World Haptics Conference*, pages 263–268.

[Verrillo and Gescheider, 1983] Verrillo, R. and Gescheider, G. (1983). Vibrotactile masking: Effects of one-and two-site stimulation. *Perception & Psychophysics*, 33(4):379–387.

[Vezzoli et al., 2014] Vezzoli, E., Amberg, M., Giraud, F., and Lemaire-Semail, B. (2014). Electrovibration modeling analysis. In *Proc. of the 9th International Conference, Eurohaptics 2014*, pages 369–376, Versailles, France.

[Vodlak et al., 2016] Vodlak, T., Vidrih, Z., Vezzoli, E., Lemaire-Semail, B., and Peric, D. (2016). Multi-physics modelling and experimental validation of electrovibration based haptic devices. *Biotribology*, (37).

[Wang et al., 2016] Wang, Q., Ren, X., Sarcar, X., and Sun, X. (2016). Ev-pen: Leveraging electrovibration haptic feedback in pen interaction. In *ISS '16, Proceedings of the 2016 ACM on Interactive Surfaces and Spaces*, pages 57–66.

[Watabene and Fukui, 1995] Watabene, T. and Fukui, S. (1995). Method for controlling tactile sensation of surface roughness using ultrasonic vibration. In *IEEE International Conference on Robotics and Automation*, pages 1134–1139.

[Wiertlevski and Hayward, 2012] Wiertlevski, M. and Hayward, V. (2012). Mechanical behavior of the fingertip in the range of frequencies and displacements relevant to touch. *Journal of Biomechanics*, 45:1869–1874.

[Wijekoon et al., 2012] Wijekoon, D., Cecchinato, M., Hoggan, E., and Linjama, J. (2012). Electrostatic modulated friction as tactile feedback: Intensity perception. In *Haptics: Perception, Devices, Mobility, and Communication Lecture Notes in Computer Science*, volume 7282, pages 613–624.

[Winfield et al., 2008] Winfield, L., Glassmire, J., Colgate, J., and Peshkin, M. (2008). T-pad: Tactile pattern display through variable friction reduction. In *IEEE World Haptics Conference*, pages 421–426.

[Xu et al., 2012] Xu, C., Israr, A., Bau, O., Kim, S., and Poupyrev, I. (2012). Tactile feedback on flat surfaces for the visually impaired. In *CHI'12*, pages 1571–1576.

[Yamamato et al., 2006] Yamamato, A., Nagasawa, S., Yamamato, H., and Higuchi, T. (2006). Electrostatic tactile display with thin film slider and its application to tactile tele-presentation system. *IEEE Transactions on Visualization and Computer Graphics*, 12(2):168–176.

[Yamamoto and Yamamoto, 1976] Yamamoto, T. and Yamamoto, Y. (1976). Dielectric constant and resistivity of epidermal stratum corneum. *Medical and Biological Engineering*, pages 494–500.

[Yıldız and Güçlü, 2013] Yıldız, M. and Güçlü, B. (2013). Relationship between vibrotactile detection threshold in the pacinian channel and complex mechanical modulus of the human glabrous skin. *Somatosensory & Motor Research*, 30:37–47.

[Yıldız et al., 2015] Yıldız, M., Toker, İ., Özkan, F., and Güçlü, B. (2015). Effects of passive and active movement on vibrotactile detection thresholds of the pacinian channel and forward masking. *Somatosensory & Motor Research*, 32(4):262–272.

[Yoshioka et al., 2007] Yoshioka, T., Craig, J., Beck, G., and Hsiao, S. (2007). Perceptual constancy of texture roughness in the tactile system. *The Journal of Neuroscience*, 31(48):1760317611.

[Zwislocki and Relkin, 2001] Zwislocki, J. and Relkin, E. M. (2001). On a psychophysical transformed-rule up and down method converging on a 75 % level of correct responses. *Proceedings of the National Academy of Sciences of the United States of America*, 98(8):4811–4814.

VITA

Yasemin Vardar was born in Ankara, Turkey, on September 21, 1987. She is currently a Ph.D. candidate in Mechanical Engineering at Koç University, Istanbul. She received her B.Sc. degree in Mechatronics Engineering from Sabanci University, Istanbul in 2010. Then, she received her M.Sc. degree in Systems and Control from Eindhoven University of Technology in 2012. Before starting her Ph.D. study, she conducted research on control of high precision systems in ASML, Philips, and TNO Eindhoven. Her research interests are haptic science and applications, mechatronics, and control.